

# Global CFFs fit with Neural Networks: Toward dispersion relation constraints and D-term extraction

Melany Higuera-Angulo

In collaboration with Alexandre Camsonne, Volker Burkert, David Richards, Daniel Lersch,  
Pierre Chatagnon.



Vector Quarkonia as Pressure Gauges  
Jefferson Lab, Newport News, Virginia  
March 27th, 2026



# Outline

## 1. Motivation:

- Mechanical properties of the proton.
- From observables to Compton form factors.

## 2. Framework:

- Gepar + Neural Networks
- Extraction of CFFs from experimental data using NN.

## 3. State of the analysis:

- Model stability: Closure test.
- Update on global analysis of CFFs.
- Dispersion relation and D-term extraction roadmap.

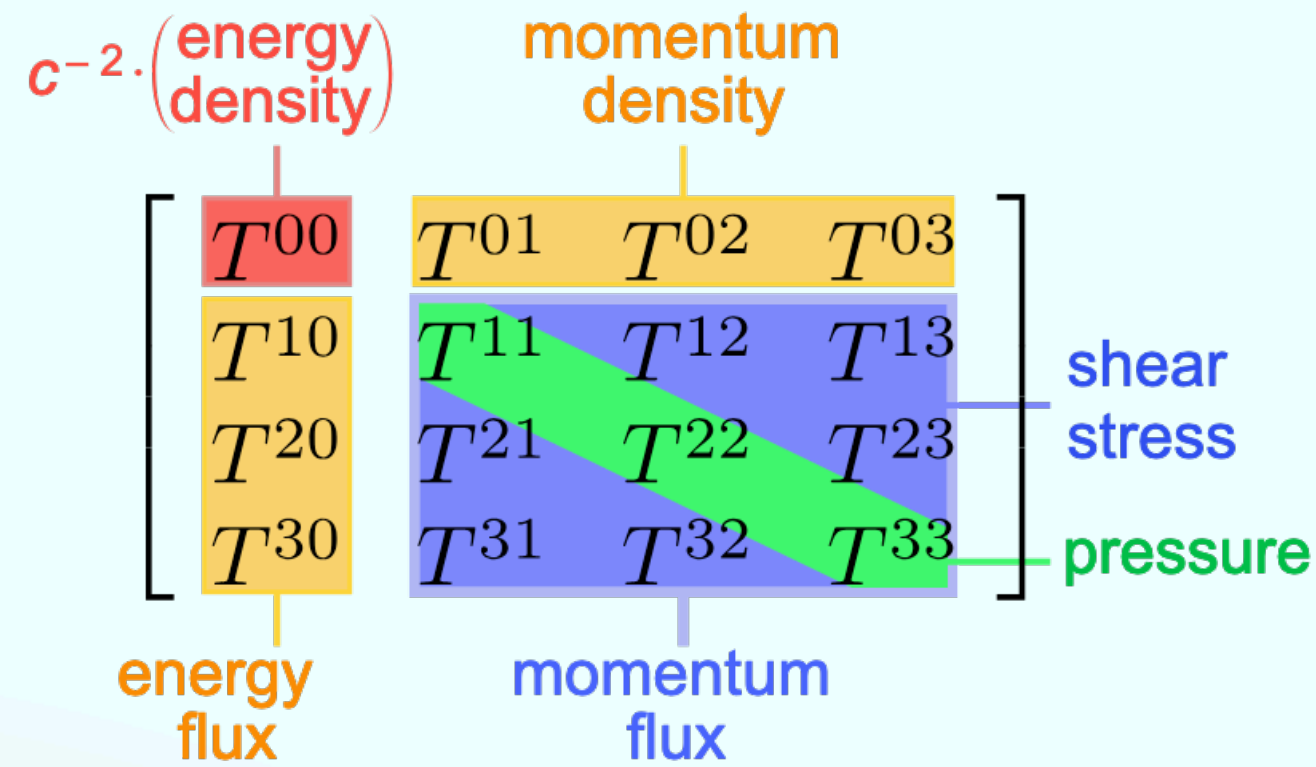
## 4. Deliverables and future directions

# Motivation and scope of the project:

- Mechanical properties of the proton.
- From DVCS observables to Compton form factors

# Mechanical properties of the proton

The Matrix element of the QCD Energy-Momentum tensor encodes key information of the proton including the mass and spin, as the distributions of energy, angular momentum, and various mechanical properties such as, e.g., internal forces inside the system.



$$\langle p', \vec{s}' | T_a^{\mu\nu} | p, \vec{s} \rangle = \bar{u}(p', \vec{s}') \left[ A_a(t) \frac{P^\mu P^\nu}{M_N} + D_a(t) \frac{\Delta^\mu \Delta^\nu - g^{\mu\nu} \Delta^2}{4M_N} + \bar{C}_a(t) M_N g^{\mu\nu} + J_a(t) \frac{P^{\{\mu} i \sigma^{\nu\} \lambda} \Delta_\lambda}{M_N} - S_a(t) \frac{P^{[\mu} i \sigma^{\nu] \lambda} \Delta_\lambda}{M_N} \right] u(p, \vec{s})$$

Momentum
Pressure
Total angular momentum

Symmetric kinematical variables:

$$P = (p' + p)/2 \text{ and } \Delta = p' - p$$

Free Dirac spinor:

$$u(p, \vec{s})$$

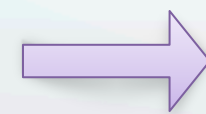
GFFs:  $A_a(t), D_a(t), \bar{C}_a(t), \text{ and } J_a(t)$

On top of restricting the number of GFFs, Poincaré symmetry imposes additional constraints:

$$\begin{aligned} A(0) &= \sum_q A_q(0) + A_G(0) = 1, \\ J(0) &= \sum_q J_q(0) + J_G(0) = \frac{1}{2}, \\ \frac{1}{2} \Delta \Sigma &= \sum_q S_q(0), \\ \bar{C}(t) &= \sum_q \bar{C}_q(t) + \bar{C}_G(t) = 0, \end{aligned}$$

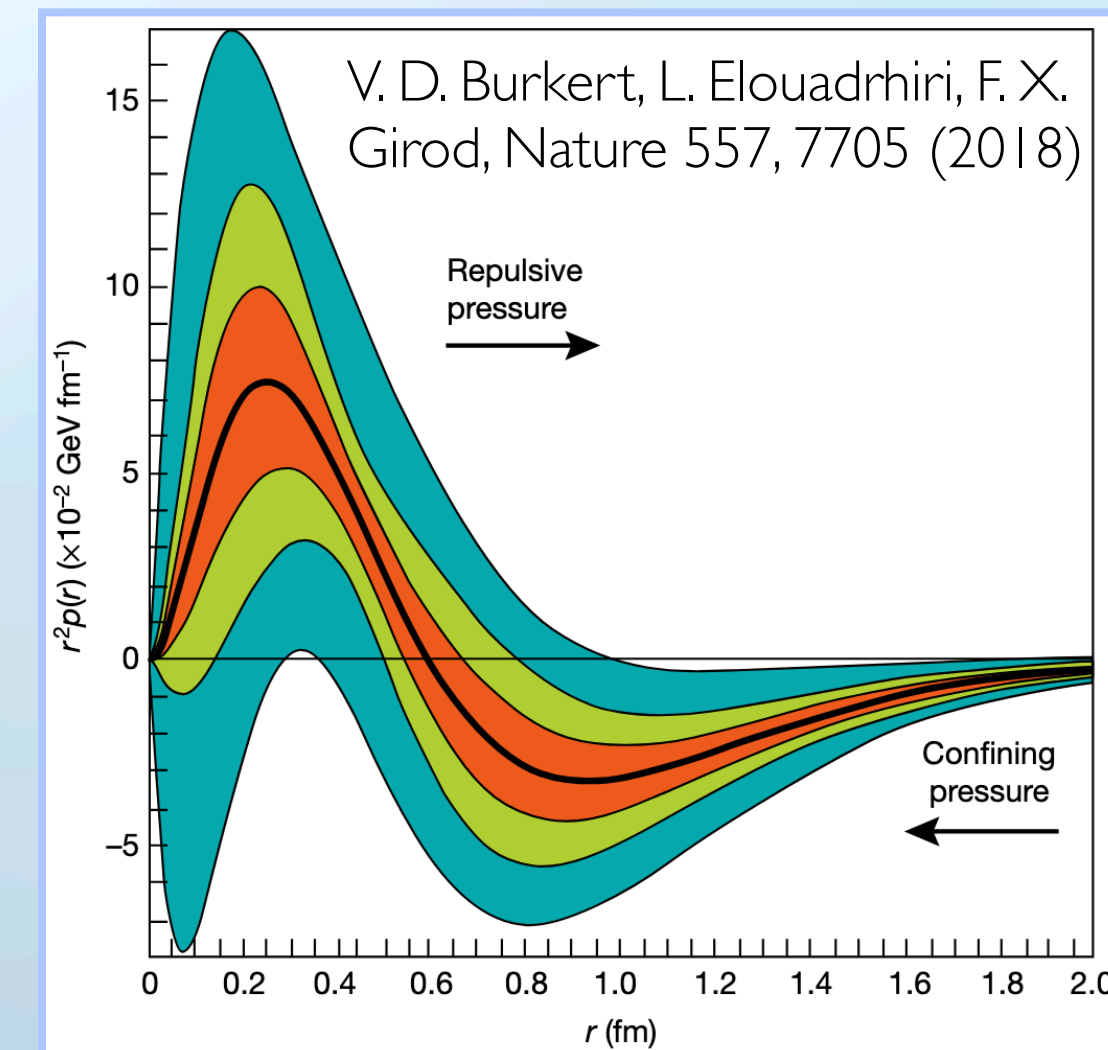
$D(t)$  is the lesser-known GFF. Its value is not fixed by spacetime symmetries and must be determined from experiment.

$$D(t) = ?$$



$$\Delta(t) \propto D(t) \propto \int d^3\mathbf{r} p(r) \frac{j_0(r\sqrt{-t})}{t}$$

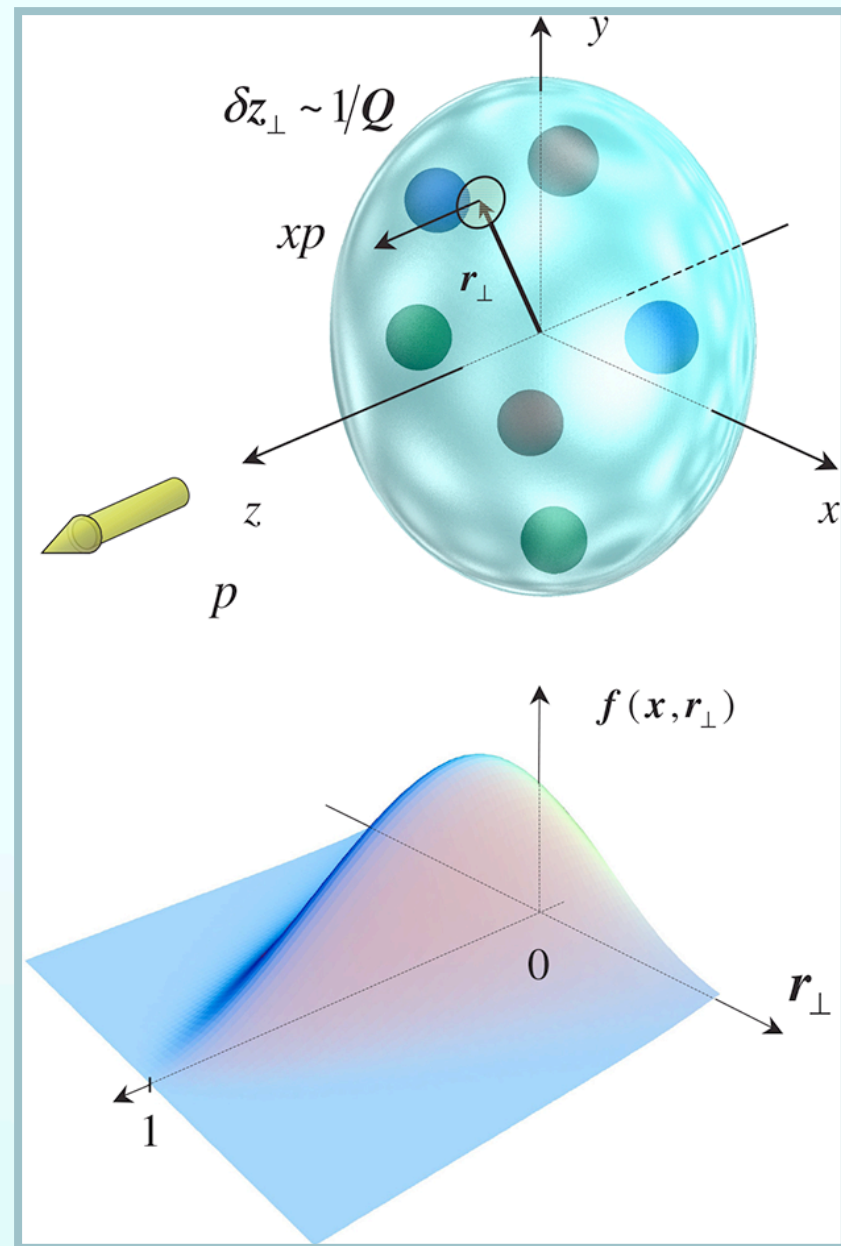
The D-term is not related to “external properties” of a particle like mass and spin, but to the stress tensor and internal force.



# From DVCS observables to Compton form factors

The DVCS amplitude depends on the complex-valued convolution integrals of the **GPDs**: **Compton form factors (CFFs)**

We cannot access GPDs directly



$$\int_{-1}^1 dx x H^q(x, \xi, t) = A^q(t) + \xi^2 D^q(t)$$

$$\int_{-1}^1 dx x E^q(x, \xi, t) = B^q(t) - \xi^2 D^q(t)$$

twist 2 GPDs:  $\{H, E, \tilde{H}, \tilde{E}\}$

Thanks to the DVCS LO, it is possible to obtain the fixed-t dispersion relation (DR) where the subtraction constant is related to the so-called **D-term**.

$$\text{Re}\mathcal{H}(\xi, t) + i \text{Im}\mathcal{H}(\xi, t) = \sum_q e_q^2 \int_{-1}^1 dx \left[ \frac{1}{\xi - x - i\epsilon} - \frac{1}{\xi + x - i\epsilon} \right] H_q(x, \xi, t)$$

$\xi = x_B / (2 - x_B)$  is the skewness variable  
 $x_B$  is the Bjorken scaling variable  
 $t$  is the squared momentum transfer to the nucleon.

- The inverse problem is intrinsically ill-posed.

Subtraction constant

$$\text{Re}\mathcal{H}(\xi, t) = \Delta(t) + \frac{1}{\pi} \text{P.V.} \int_0^1 d\xi' \left[ \frac{1}{\xi - \xi'} - \frac{1}{\xi + \xi'} \right] \text{Im}\mathcal{H}(\xi', t)$$

Where

$$\Delta(t) = 2 \sum_q e_q^2 \int_{-1}^1 dz \frac{D_{\text{term}}^q(z, t)}{1 - z}$$

$$D_{\text{term}}^q(z, t) = (1 - z^2) \sum_{\text{odd } n} d_n^q(t) C_n^{3/2}(z)$$

1. At leading order, we assume the subtraction constant is dominantly coming from quarks.
2. In the asymptotic limit  $d_n^q(t)$  vanish for  $n > 1$ .
3. Dominance of the flavor singlet combination.

$$\rightarrow D^Q(t) = \frac{18}{25} \Delta(t)$$

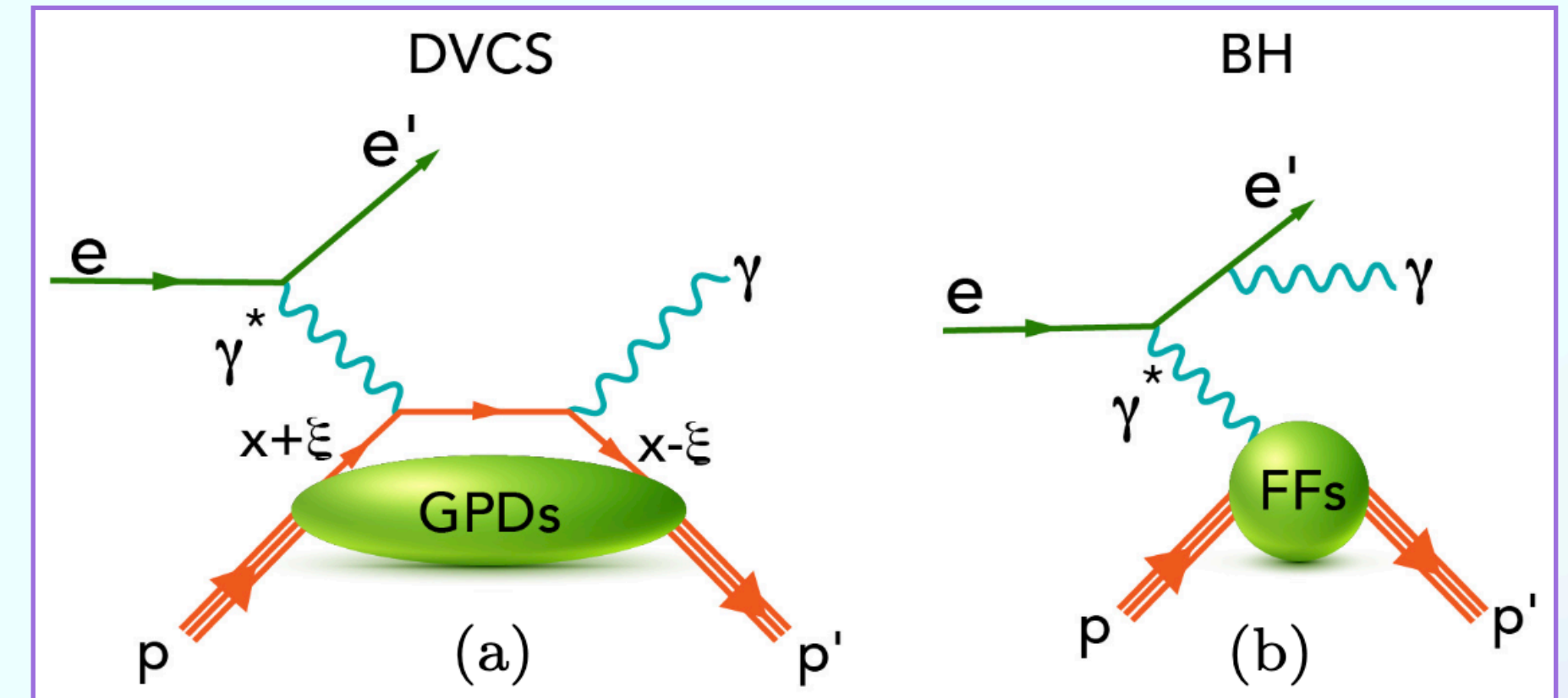
# From DVCS observables to Compton form factors

Measurements of DVCS are mostly realized via the process of lepton production of a real photon, where also an interference with the Bethe-Heitler radiation also occurs

The BH process gives access to elastic form factors, it does not see the 3D structure of hadrons.

$$\frac{d^5\sigma}{dx_B dQ^2 d|t| d\phi d\phi_S} = \frac{\alpha^3 x_B}{16\pi^2 Q^4 \sqrt{1+\epsilon^2}} |\mathcal{T}|^2,$$

$$|\mathcal{T}|^2 = |\mathcal{T}_{\text{BH}} + \mathcal{T}_{\text{DVCS}}|^2 = |\mathcal{T}_{\text{BH}}|^2 + |\mathcal{T}_{\text{DVCS}}|^2 + \mathcal{I}.$$



The interference is actually what gives us strong sensitivity to the CFFs. The DVCS amplitude can be decomposed either in helicity amplitudes or, equivalently, in complex valued CFFs.

$$|\mathcal{T}_{\text{DVCS}}|^2 = \frac{2(2-2y+y^2)}{y^2 Q^2 (2-x_B)^2} \left[ 4(1-x_B) (|\mathcal{H}|^2 + |\tilde{\mathcal{H}}|^2) - \left( x_B^2 + (2-x_B)^2 \frac{\Delta^2}{4M^2} \right) |\mathcal{E}|^2 - x_B^2 \left( \mathcal{H}\mathcal{E}^* + \mathcal{E}\mathcal{H}^* + \tilde{\mathcal{H}}\tilde{\mathcal{E}}^* + \tilde{\mathcal{E}}\tilde{\mathcal{H}}^* \right) - x_B^2 \frac{\Delta^2}{4M^2} |\tilde{\mathcal{E}}|^2 \right], \quad y = \frac{Q^2}{xs}.$$

BMK equations relate the CFFs to measurable quantities such as  $\Delta^4\sigma, d^4\sigma, A_{LU}, A_{UL}, A_C, A_{LL} \dots$

The first sine harmonic of the beam spin asymmetry (BSA), as measured e.g. in Jefferson Lab is defined as:

• Beam spin asymmetry:  $A_{LU}^{-, \sin \phi} \equiv \frac{1}{\pi} \int_{-\pi}^{\pi} d\phi \sin \phi A_{LU}^{-}(\phi)$

The CFFs are the direct bridge between theory and measurable data. →

For truly Global analysis, the CFFs are usually indirectly modeled by GPDs models. However, we don't do that.

# Experimental observables

## Observables used:

- Beam spin difference cross section:

$$\Delta^4\sigma = \frac{1}{2} \left[ \frac{d^4\sigma(\lambda = +1)}{dQ^2 dx_B dt d\phi} - \frac{d^4\sigma(\lambda = -1)}{dQ^2 dx_B dt d\phi} \right]$$

- Beam spin sum cross section:

$$d^4\sigma = \frac{1}{2} \left[ \frac{d^4\sigma(\lambda = +1)}{dQ^2 dx_B dt d\phi} + \frac{d^4\sigma(\lambda = -1)}{dQ^2 dx_B dt d\phi} \right]$$

- Beam charge asymmetry:

$$A_C = \frac{\sigma_{UU}^+ - \sigma_{UU}^-}{\sigma_{UU}^+ + \sigma_{UU}^-} \propto \Re \left[ F_1 \mathcal{H} + \xi (F_1 + F_2) \widetilde{\mathcal{H}} - \frac{\Delta^2}{4M^2} F_2 \mathcal{E} \right] \cos \phi$$

- Beam spin asymmetry:

$$A_{LU}(\phi) = \frac{d\sigma^\uparrow(\phi) - d\sigma^\downarrow(\phi)}{d\sigma^\uparrow(\phi) + d\sigma^\downarrow(\phi)} \propto \Im \left\{ F_1 \mathcal{H} + \xi (F_1 + F_2) \widetilde{\mathcal{H}} - \frac{\Delta^2}{4M^2} F_2 \mathcal{E} \right\} \sin(\phi)$$

- Target spin asymmetry:

$$A_{UL}(\phi) = \frac{d\sigma^\Rightarrow(\phi) - d\sigma^\Leftarrow(\phi)}{d\sigma^\Rightarrow(\phi) + d\sigma^\Leftarrow(\phi)} \propto \Im \left[ F_1 \widetilde{\mathcal{H}} + \xi (F_1 + F_2) \left( \mathcal{H} + \frac{x_B}{2} \mathcal{E} \right) - \xi \left( \frac{x_B}{2} F_1 + \frac{t}{4M^2} F_2 \right) \widetilde{\mathcal{E}} \right] \sin(\phi)$$

- Double spin asymmetry:

$$A_{LL}(\phi) = \frac{d\sigma^{\uparrow\uparrow}(\phi) - d\sigma^{\downarrow\uparrow}(\phi) - d\sigma^{\uparrow\downarrow}(\phi) + d\sigma^{\downarrow\downarrow}(\phi)}{d\sigma^{\uparrow\uparrow}(\phi) + d\sigma^{\downarrow\uparrow}(\phi) + d\sigma^{\uparrow\downarrow}(\phi) + d\sigma^{\downarrow\downarrow}(\phi)} \propto \Re \left[ F_1 \widetilde{\mathcal{H}} + \xi (F_1 + F_2) \left( \mathcal{H} + \frac{x_B}{2} \mathcal{E} \right) - \xi \left( \frac{x_B}{2} F_1 + \frac{t}{4M^2} F_2 \right) \widetilde{\mathcal{E}} \right] \cos \phi + BH$$

| Collab | Year | Observable                                 | l.b.e.  | $x_B$     | $Q^2 [GeV^2]$ | $ t  [GeV^2]$ |
|--------|------|--|---------|-----------|---------------|---------------|
| CLAS   | 2001 | $A_{LU}^{sin(\phi)}$                       | 4.25    | 0.19      | 1.25          | 0.19          |
| CLAS   | 2006 | $A_{UL}^{sin(\phi)}$                       | 5.7     | 0.2-0.4   | 1.82          | 0.15-0.44     |
| CLAS   | 2007 | $A_{LU}$                                   | 5.77    | 0.13-0.35 | 1.1-3         | 0.1-0.3       |
| CLAS   | 2009 | $A_{LU}$                                   | 4.8     | 0.12-0.48 | 1.0-2.8       | 0.09-1.8      |
| CLAS   | 2015 | $A_{LU}(\phi), A_{UL}(\phi), A_{LL}(\phi)$ | 5.93    | 0.18-0.4  | 1.6-3.2       | 0.1-0.45      |
| CLAS   | 2015 | $\sigma(\phi), \Delta\sigma(\phi)$         | 5.75    | 0.1-0.58  | 1-4.6         | 0.09-0.52     |
| CLAS   | 2018 | $\sigma(\phi)$                             | 5.88    | 0.12-0.5  | 1.1-4         | 0.1-1.6       |
| CLAS   | 2023 | $A_{LU}$                                   | 10.2    | 0.09-0.45 | 1.3-6         | 0.1-2.2       |
| CLAS   | 2023 | $A_{LU}$                                   | 10.6    | 0.09-0.62 | 1.1-7.2       | 0.1-2.8       |
| CLAS   | 2026 | $\sigma(\phi)$                             | 11      | 0.72-0.5  | 1.1-5.0       | 0.12-0.91     |
| HERMES | 2001 | $A_{LU}^{sin(\phi)}$                       | 27.6    | 0.11      | 2.6           | 0.27          |
| HERMES | 2006 | $A_C^{cos(\phi)}$                          | 27.6    | 0.08-0.12 | 2.0-3.7       | 0.03-0.42     |
| HERMES | 2008 | $A_C, A_{UT,I}, A_{UT,DVCS}$               | 27.6    | 0.03-0.35 | 1-10          | <0.7          |
| HERMES | 2009 | $A_C, A_{LU,I}, A_{LU,DVCS}$               | 27.6    | 0.05-0.24 | 1.2-5.75      | <0.7          |
| HERMES | 2010 | $A_{UL}, A_{LL}$                           | 27.6    | 0.03-0.35 | 1-10          | <0.7          |
| HERMES | 2011 | $A_{LT,I}, A_{LT,BH+DVCS}$                 | 27.6    | 0.03-0.35 | 1-10          | <0.7          |
| HERMES | 2012 | $A_{LU,I}, A_{LU,DVCS}, A_C$               | 27.6    | 0.03-0.35 | 1-10          | <0.7          |
| HALL A | 2015 | $\sigma(\phi), \Delta\sigma(\phi)$         | 5.75    | 0.33-0.40 | 1.5-2.6       | 0.17-0.37     |
| HALLA  | 2017 | $\sigma(\phi), \Delta\sigma(\phi)$         | 3.3-5.5 | 0.35      | 1.51-2        | 0.18-0.36     |

Lepton-beam-energy (l.b.e.)

We made cuts at  $t=0.5 | GeV^2$ , and  $Q^2 < 1.5 GeV^2$  or  $-t/Q^2 < 0.25$

If cross-sections are measured, using weighted Fourier integrals can help to cancel the strongly oscillating Bethe-Heitler propagators and interference terms, improving the convergence of harmonic terms.

# Framework:

- Gepard + Neural Networks
- Extraction of CFFs from experimental data using NN.

# Framework: Gepard + Neural Networks

We are building upon existing tools: **Gepard**

- Python software framework dedicated to the study of GPDs.
- K. Kumerički, D. Müller, K. Passek-Kumerički, Nuclear Physics B, Volume 794, Issues 1–2, 2008

To obtain a more reliable estimate of uncertainties with reduced model dependence, we decided to utilize **Artificial Neural Networks** to parameterize the CFFs.

- Use State-of-the-art standard ML libraries.  **PyTorch**
- A tool to do a Global fit to extract CFFs and GFFs to ensure the results are driven by data.



opengpd / gpddatabase

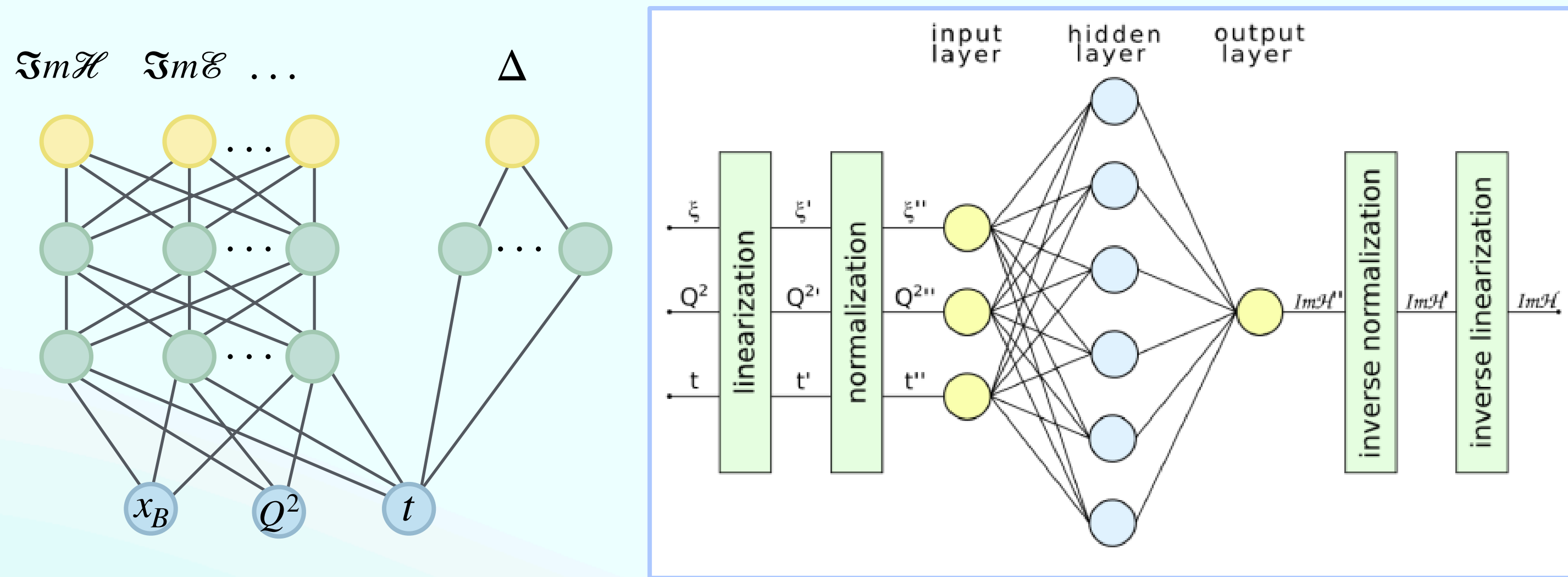
: We developed a publicly accessible database format capable of storing all current and future data, as well as pseudodata. Gepard Interface and GitHub public access; C++ & Python APIs [arxiv.org/abs/2503.18152](https://arxiv.org/abs/2503.18152)



# Extraction of CFFs from experimental data using NN

## Artificial Neural Networks (ANN)

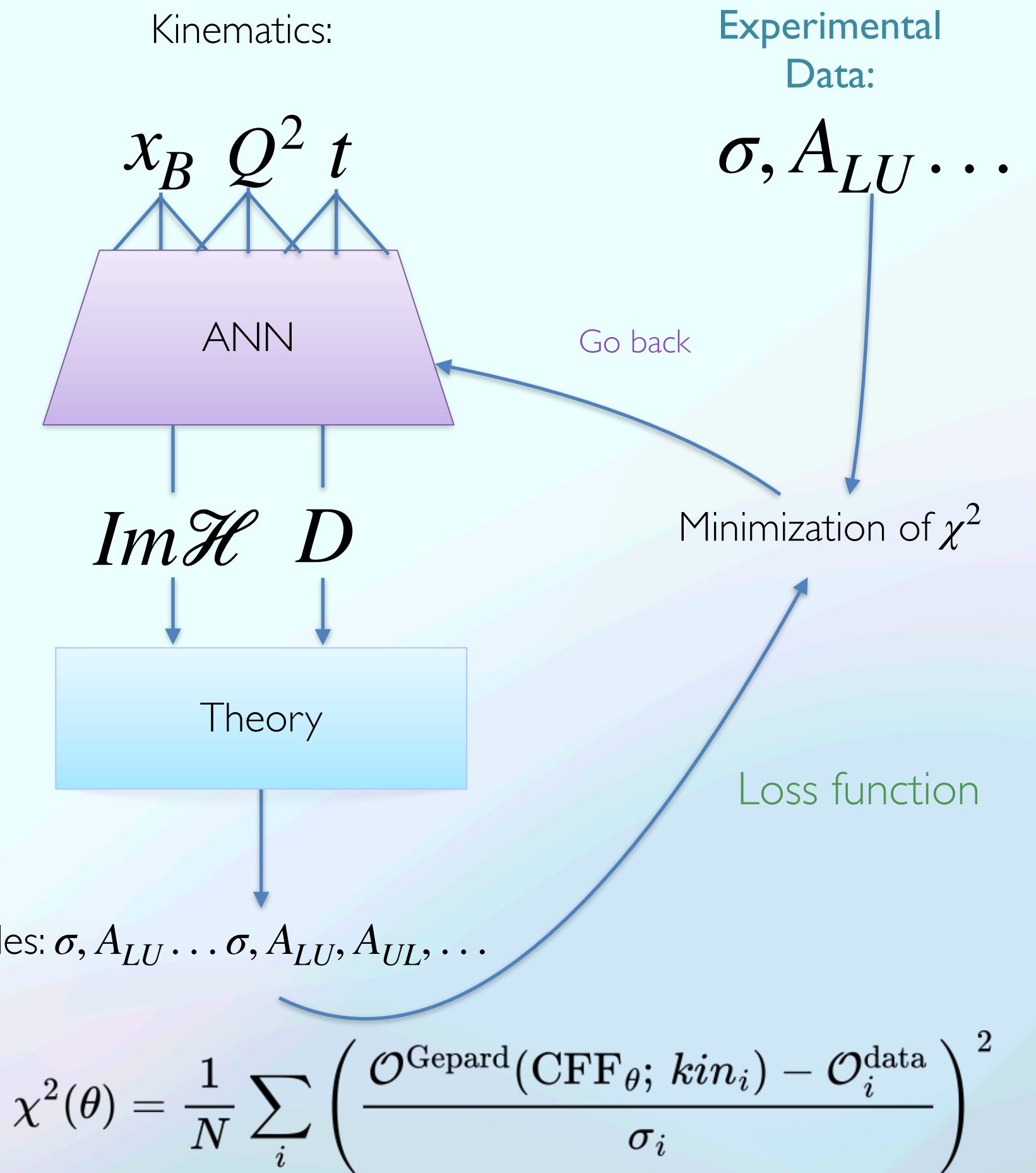
A machine learning (ML) algorithm that uses artificial intelligence (AI) to learn how to process data by analyzing training examples.



$$\text{Re}\mathcal{H}(\xi, t) = \mathcal{C}_{\mathcal{H}}(t) + \frac{1}{\pi} \text{P.V.} \int_0^1 d\xi' \left[ \frac{1}{\xi - \xi'} - \frac{1}{\xi + \xi'} \right] \text{Im}\mathcal{H}(\xi', t)$$

➔ The process is essentially a least-squares fit of a complex, multi-parameter function, implying **no theoretical bias**.

➔ For a truly global coverage, it is necessary to add a  $Q^2$  dependence, which was previously absent.



Observables:  $\sigma, A_{LU} \dots \sigma, A_{LU}, A_{UL}, \dots$

$$\chi^2(\theta) = \frac{1}{N} \sum_i \left( \frac{\mathcal{O}^{\text{Gepard}}(\text{CFF}_{\theta}; \text{kin}_i) - \mathcal{O}_i^{\text{data}}}{\sigma_i} \right)^2$$

## State of the analysis:

- Model stability and the Closure test.
- Update on global analysis of CFFs.
- Dispersion relation and D-term extraction roadmap.

# Ensemble analysis of the Neural Networks

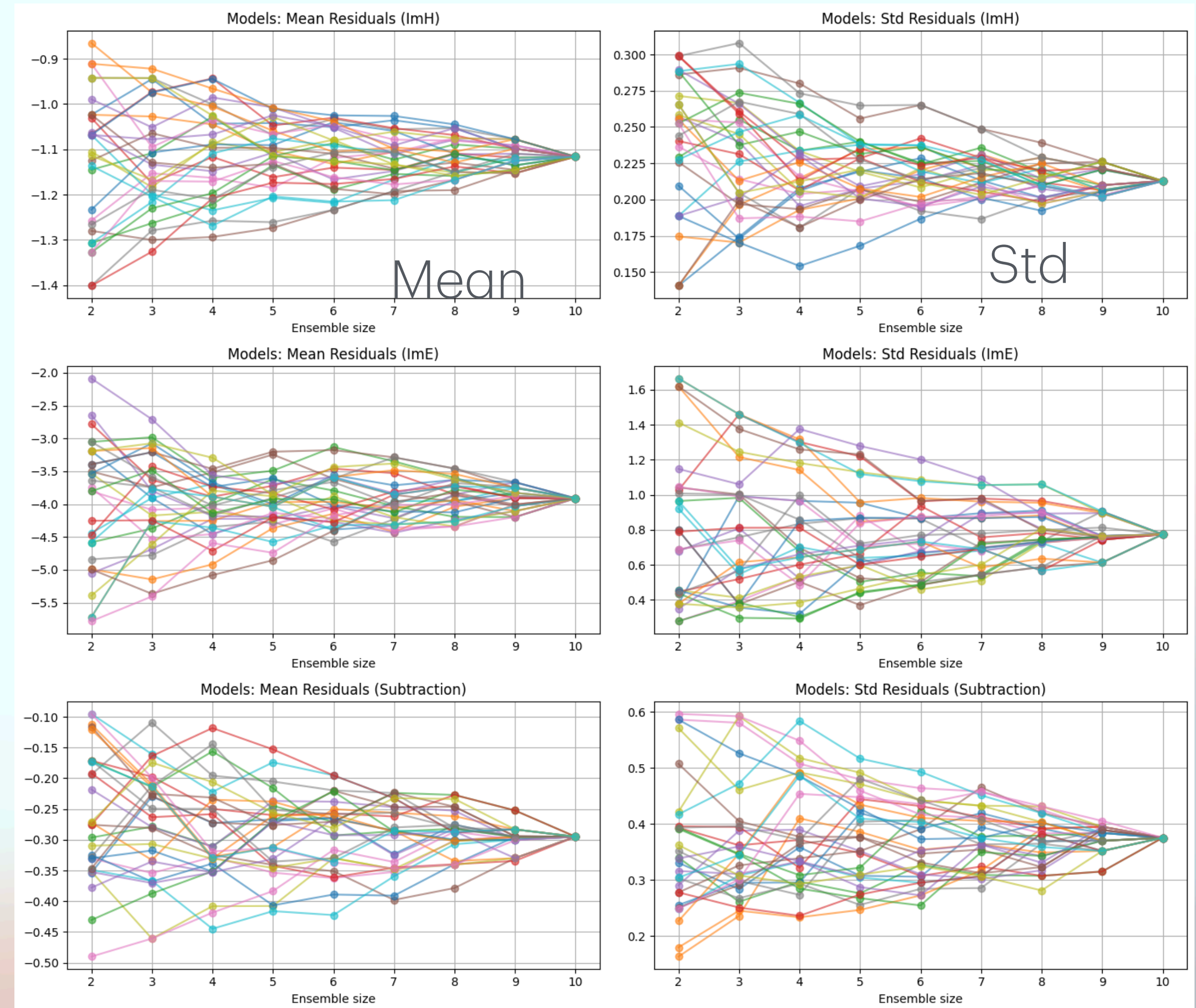
Models

To solve instability in results, we started ensemble analysis by averaging over multiple learned representations.

- To mitigate fluctuations and instability in NN results, we use an ensemble approach, averaging over multiple trained models.
- As the number of models in the ensemble increases, the mean residual prediction stabilizes, reducing noise.
- The standard deviation plots demonstrate that uncertainty decreases as the ensemble size grows.
- We can prune the results by selecting the best nets with a smaller  $\chi^2$ .

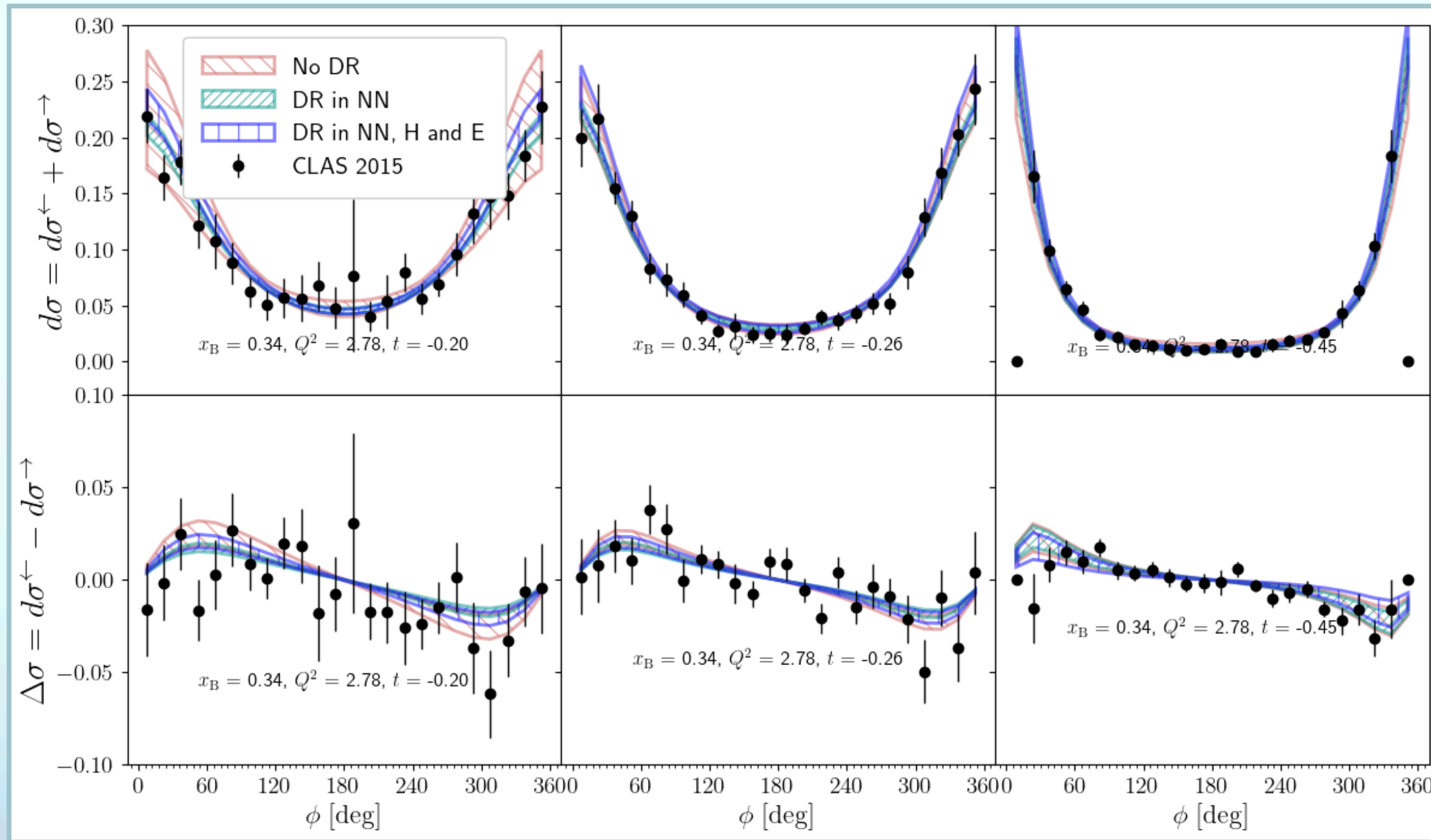
A larger ensemble tends to 'average out' individual model noise, improving the predictive stability results and uncertainty estimation of our model.

In addition, we can obtain reasonable behavior and reduce uncertainty according to the best hyperparameter selection.

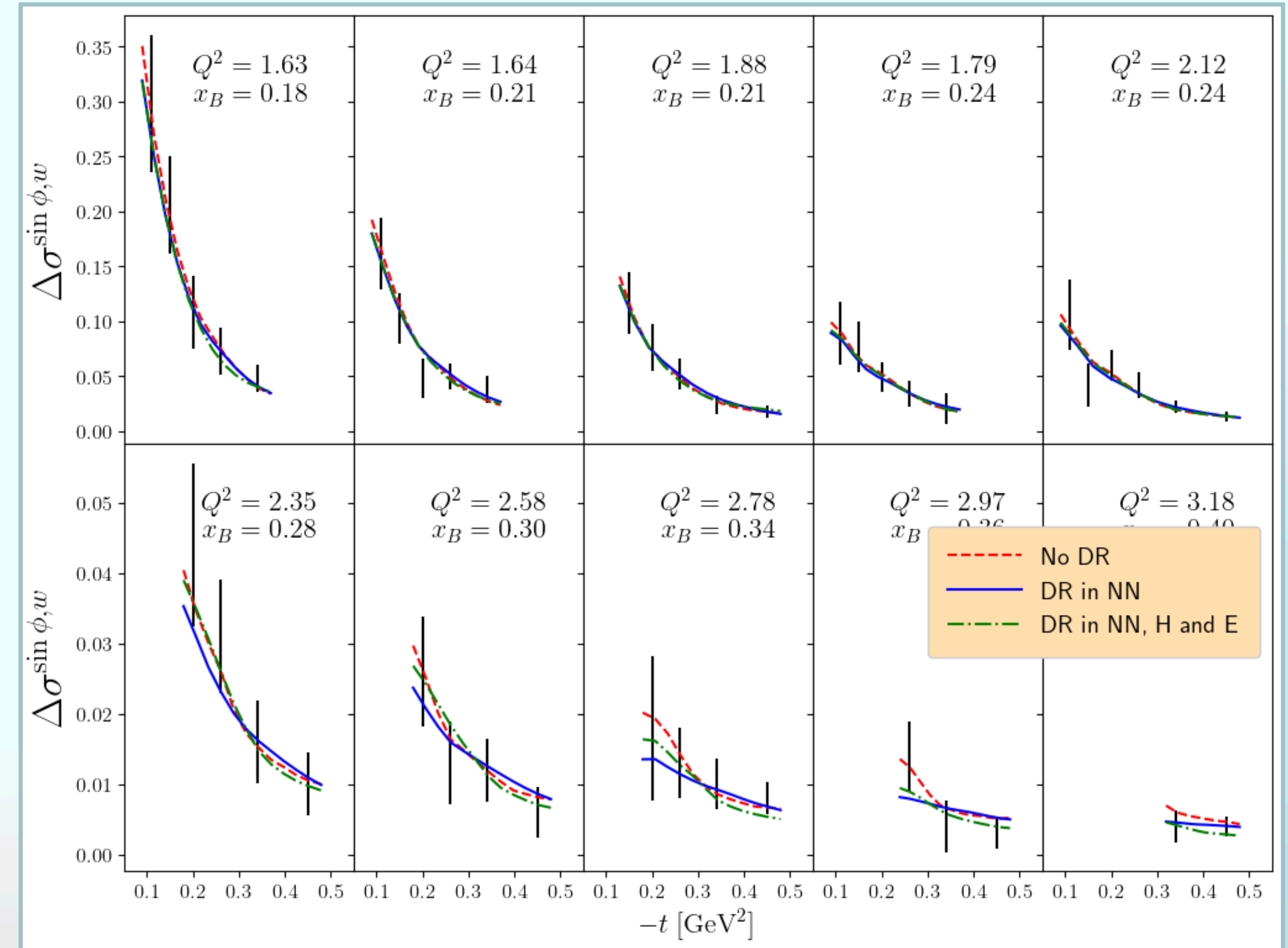


# CLAS fit

Example of description of 2015 CLAS data through the NN



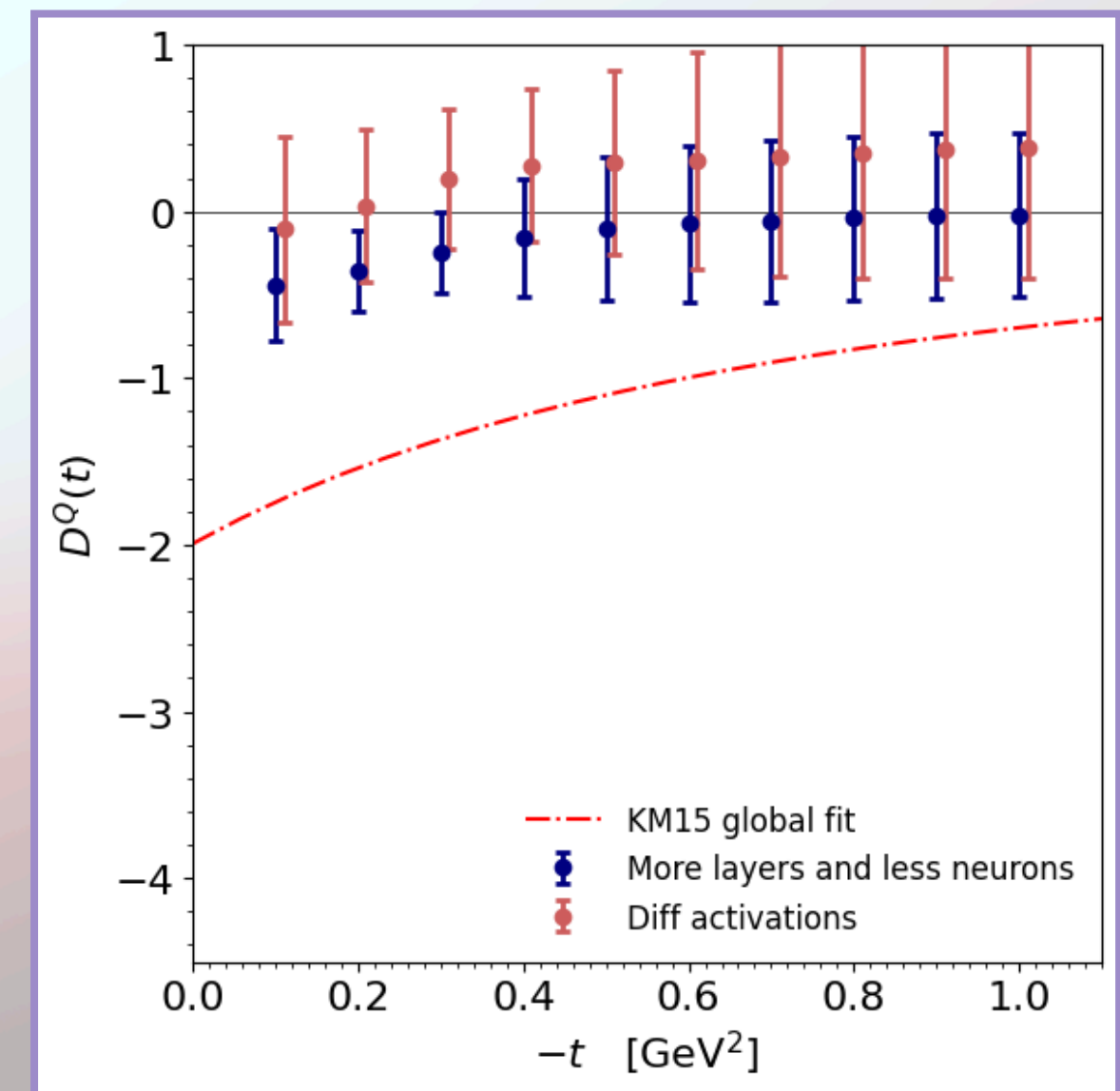
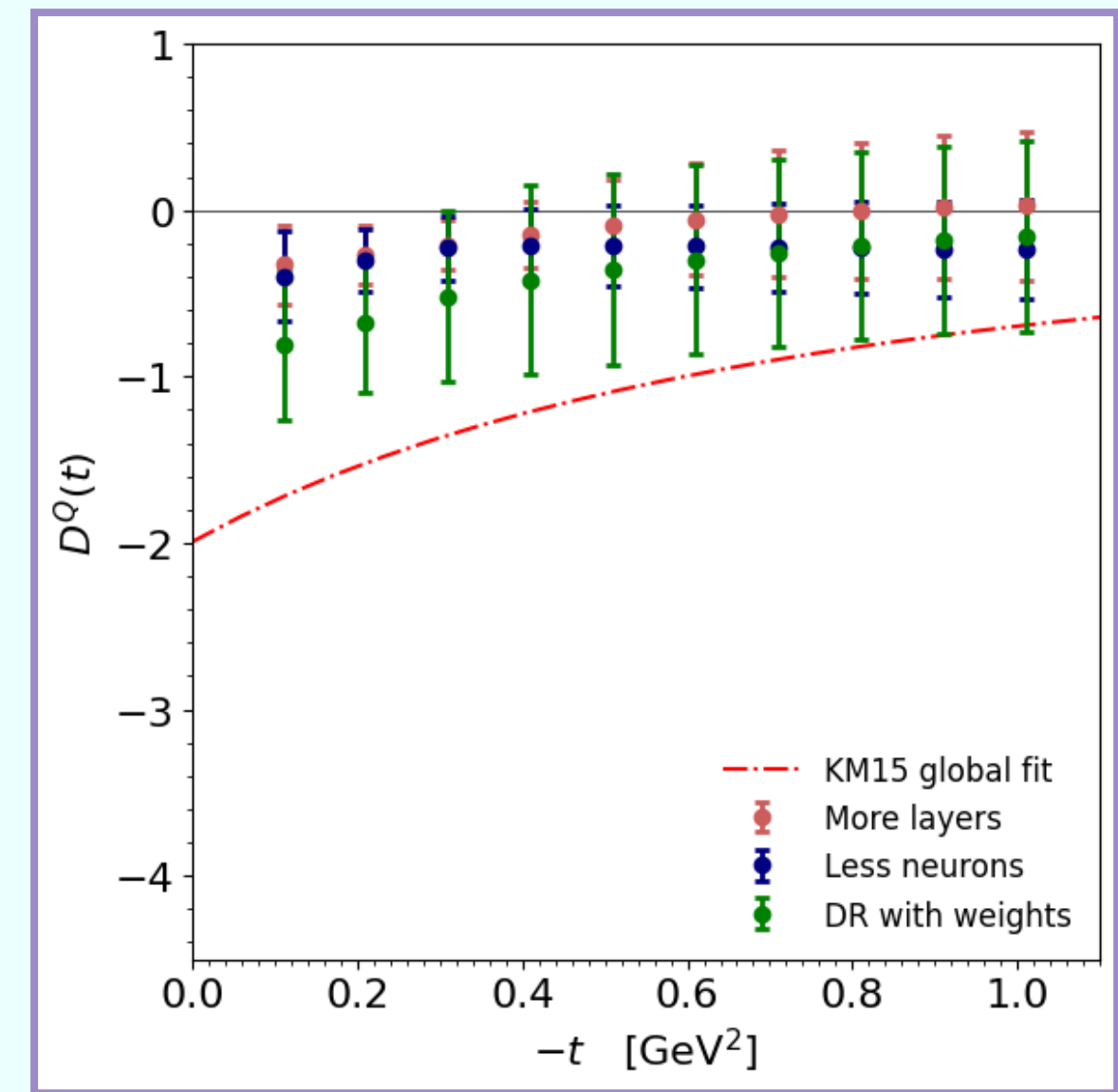
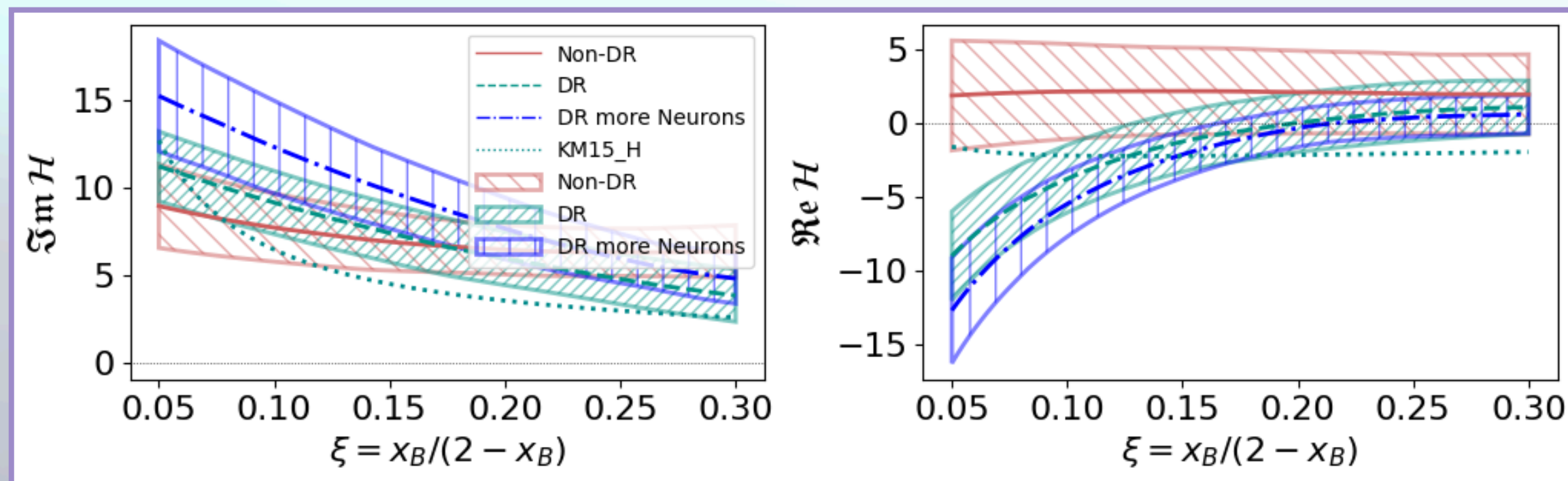
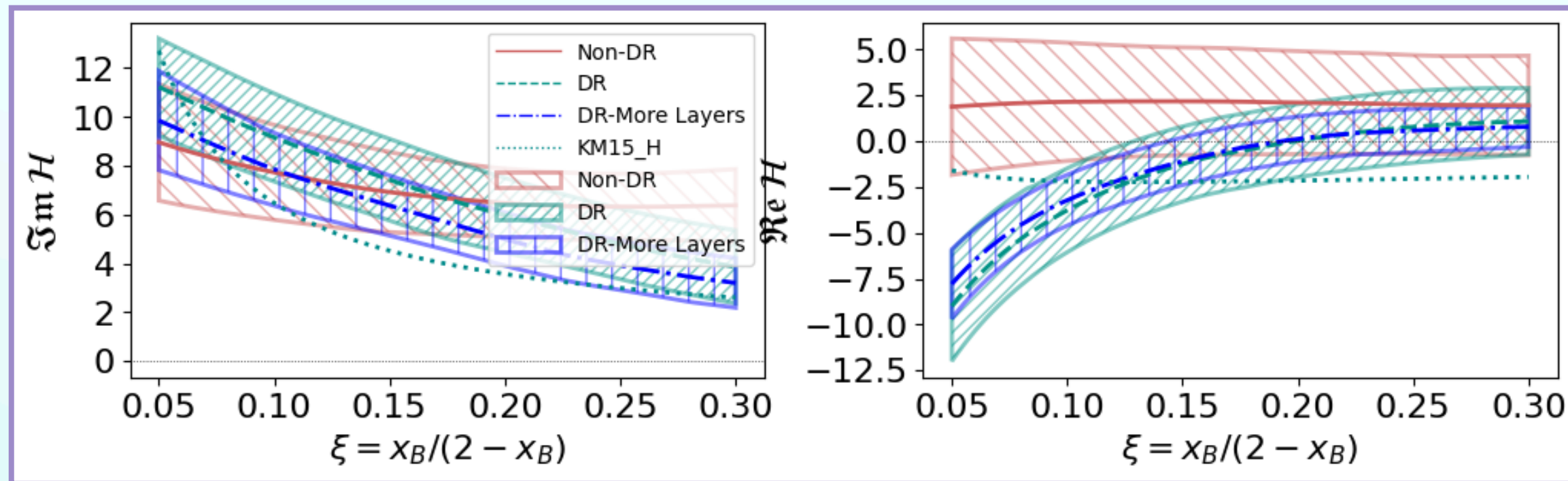
(CLAS Collaboration) Phys. Rev. Lett. 115, 212003, 2015



# Model stability (architecture dependence)

## When fitting data:

- Same dataset + same theory  $\rightarrow$  different architectures produce different  $D(t)$
- The fit was found to be very sensitive to changes. Mainly, for  $\text{Re}H$  and  $D(t)$ .



Network architecture analysis on CLAS data

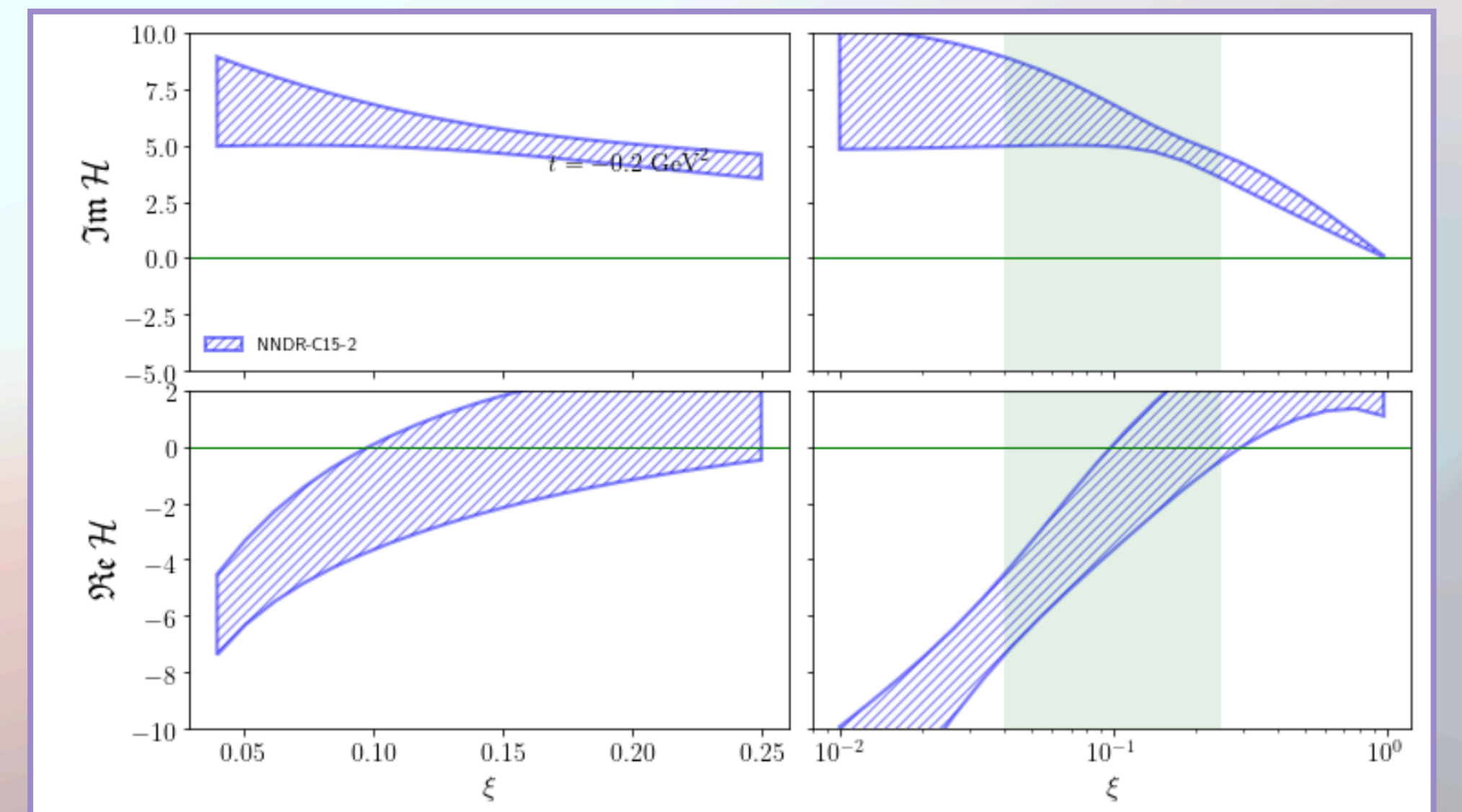
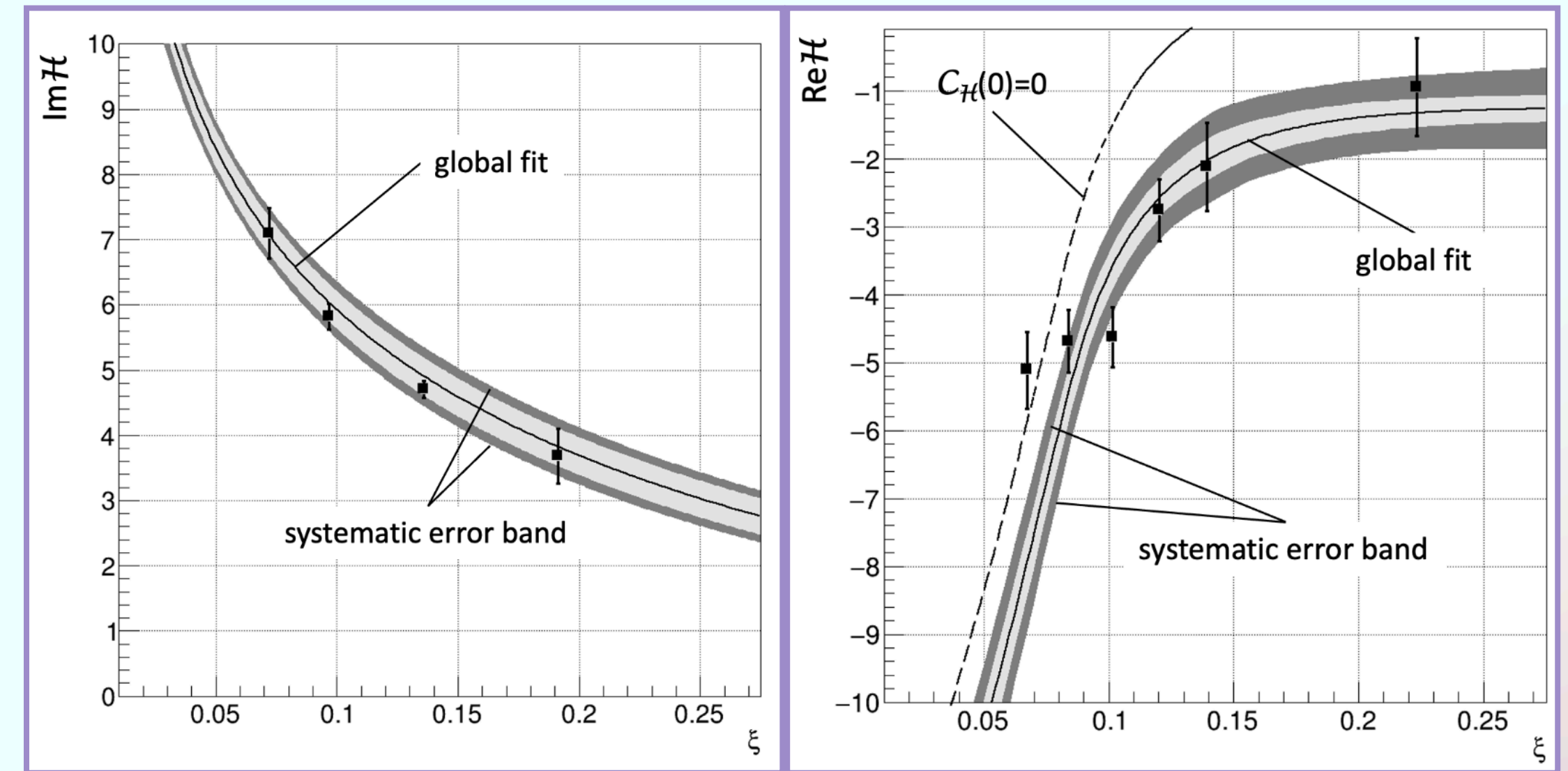
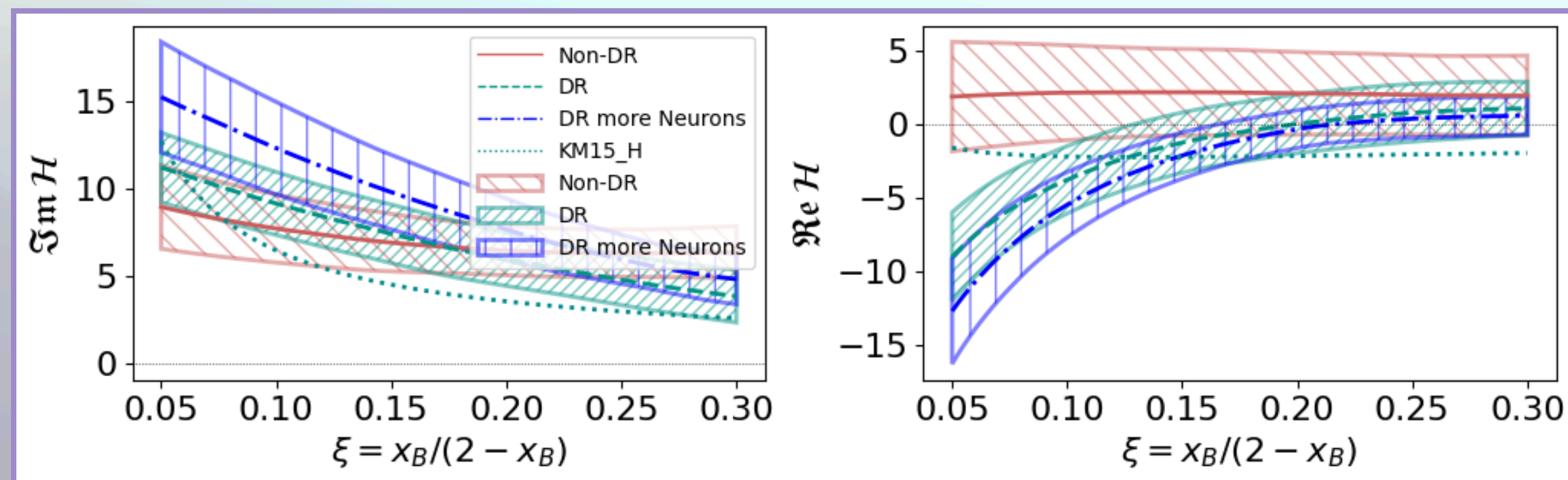
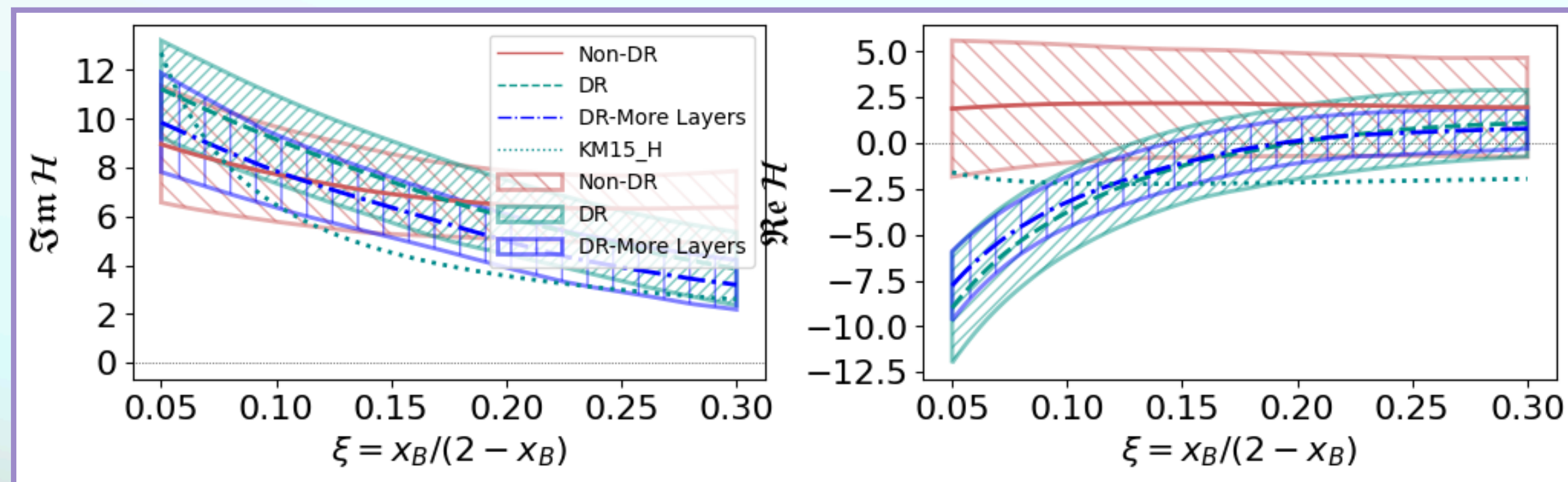
# Model stability (architecture dependence)

arXiv:2303.08347

## External consistency check using CLAS data

- Architecture choices can shift the bandwidth; we use this as a robustness check.
- Some architectures fall very close, but agreement is not used as the training criterion.

### Network architecture analysis on CLAS data



<https://github.com/openhep/dterm18/blob/master/dterm.ipynb>

# Model stability: Closure test

Our objective in the closure test is to generate pseudodata from theoretical models and verify that our neural networks can recover the original CFFs.

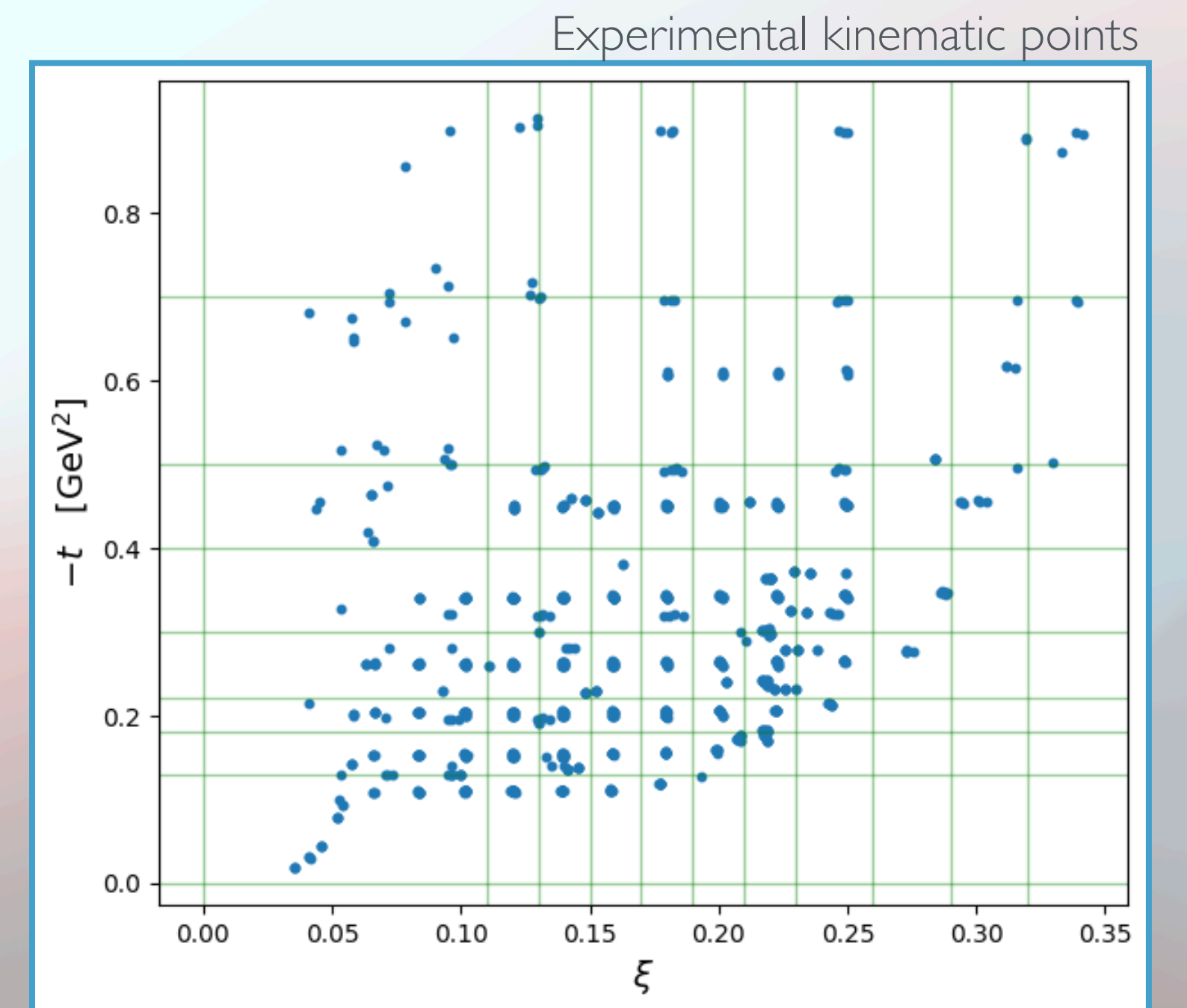
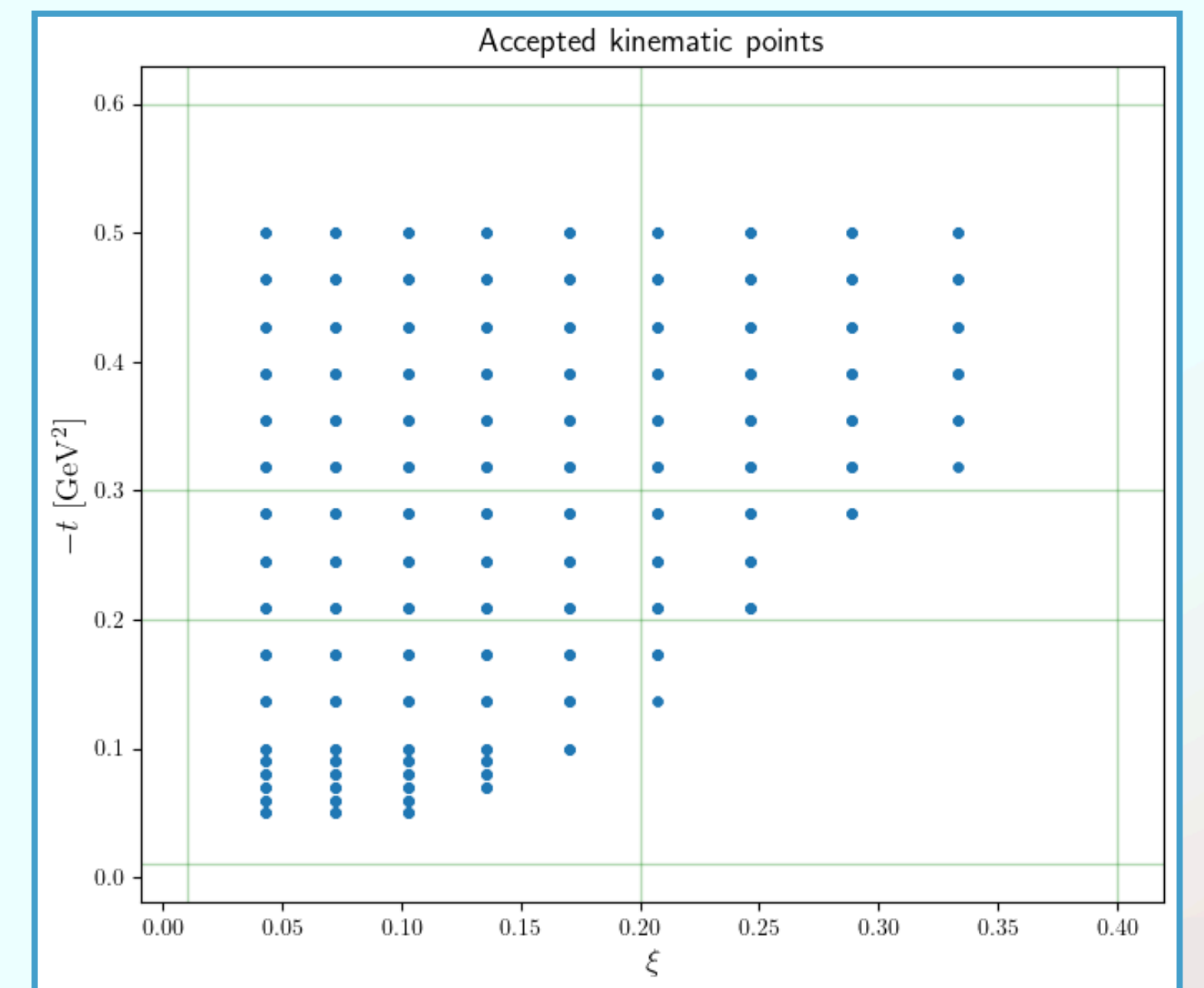
Pseudo-data must lie in the physical DVCS/BH region (BMK propagators must be real)

We fit Fourier coefficients / harmonics  $\rightarrow$  inputs are  $(x_B, Q^2, t)$ .

For fixed-target DVCS, not every combination of  $(x_B, Q^2, t)$  is allowed.

The constraints are:

- $W^2 = M^2 + Q^2(1/x_B - 1) > (M + m_\pi)^2$  (hadronic final state must exist)
- $0 < y < 1$  where  $y = \frac{\nu}{E} = \frac{Q^2}{2Mx_BE}$  (lepton energy loss fraction)
- $t_{\min}(x_B, Q^2) \leq t \leq 0$  (momentum transfer bounds)

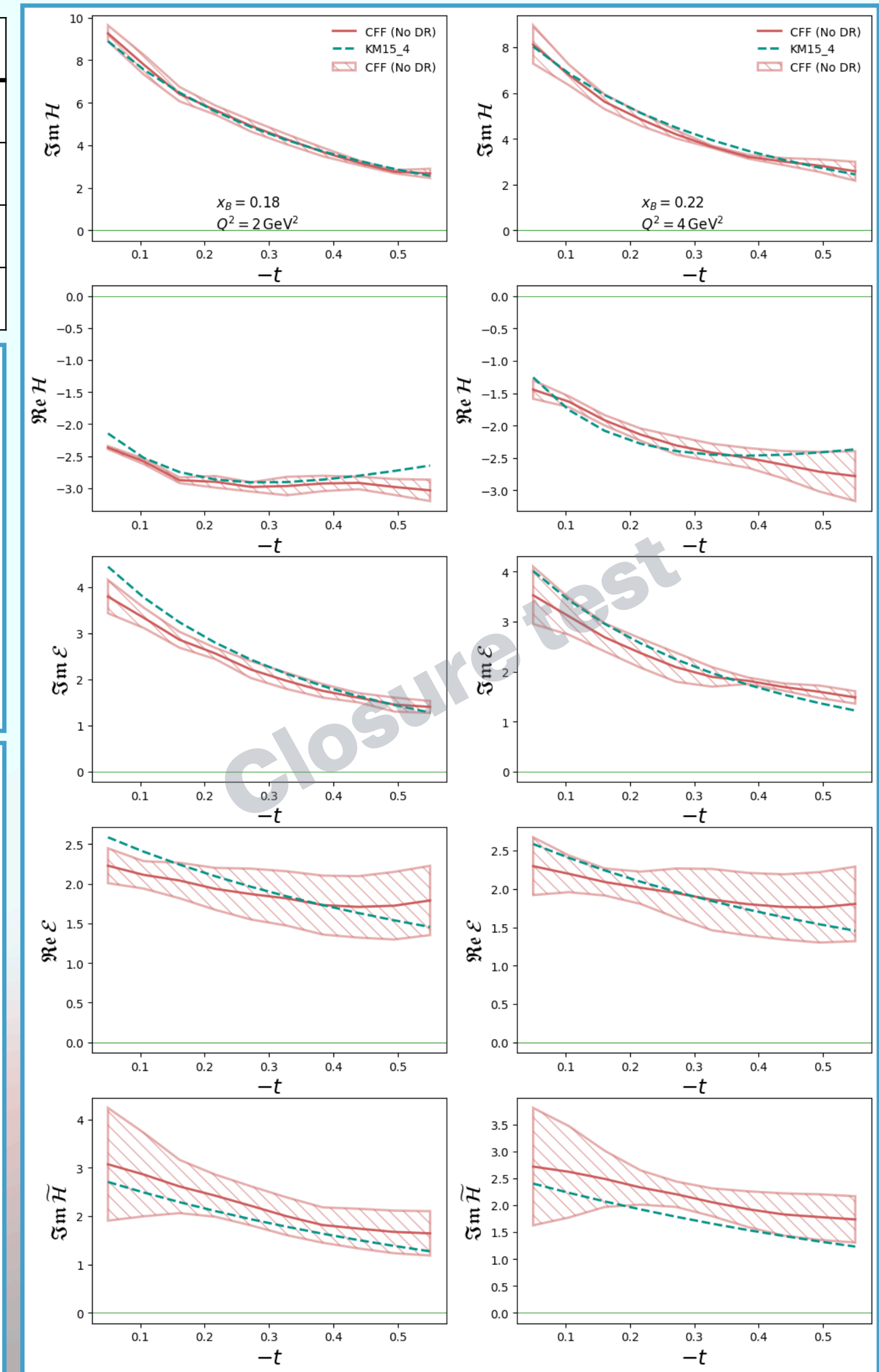
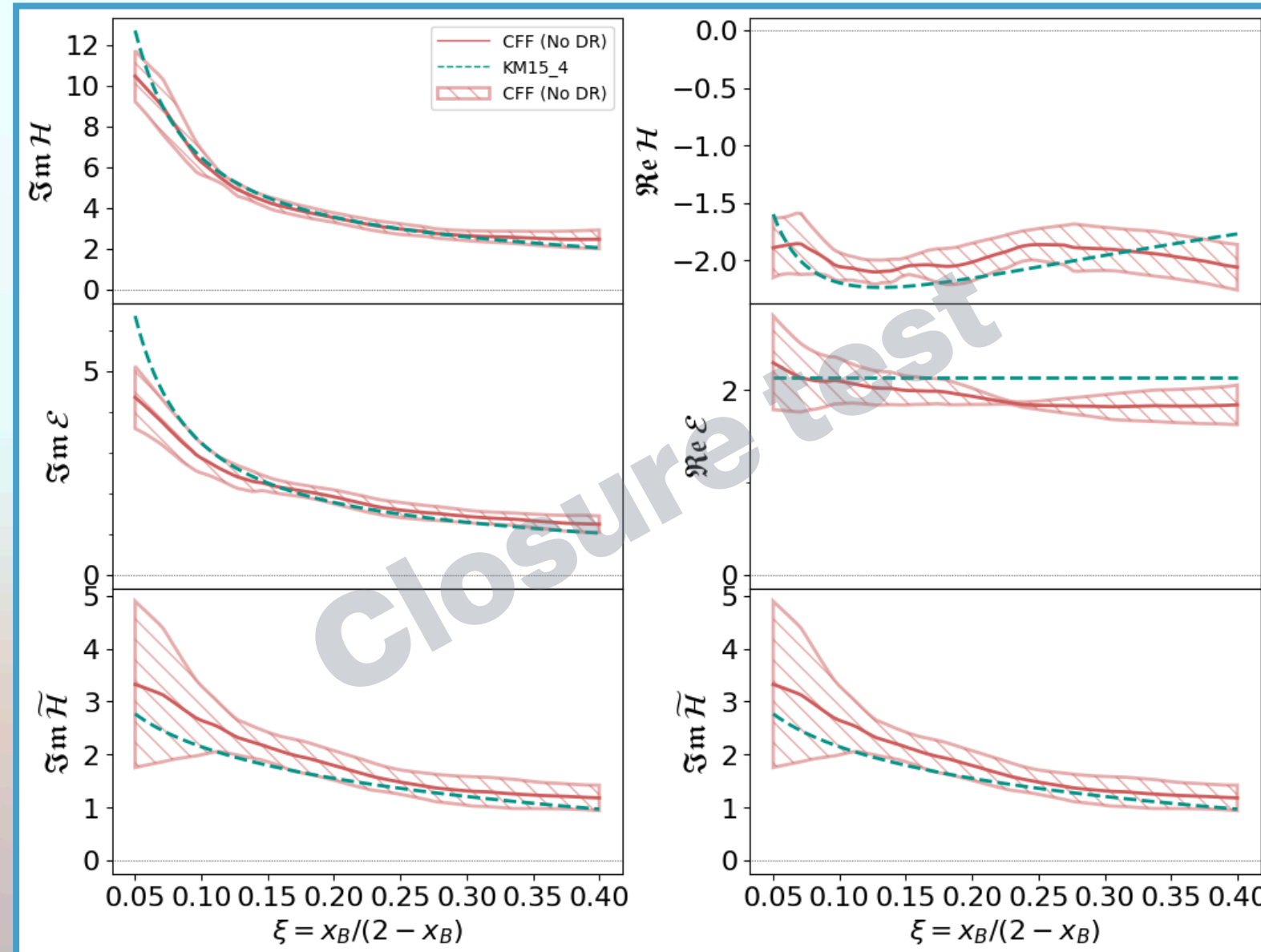
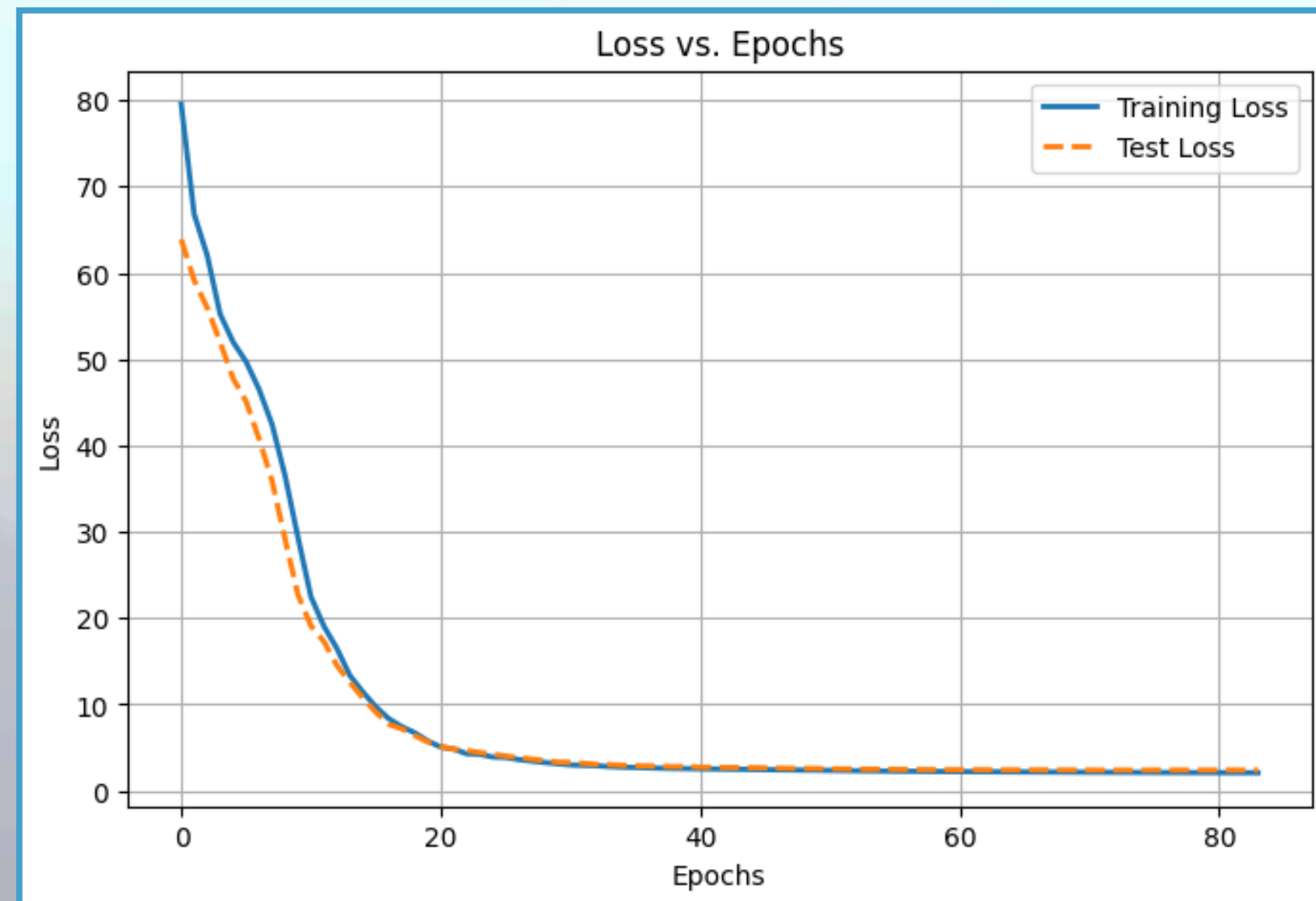
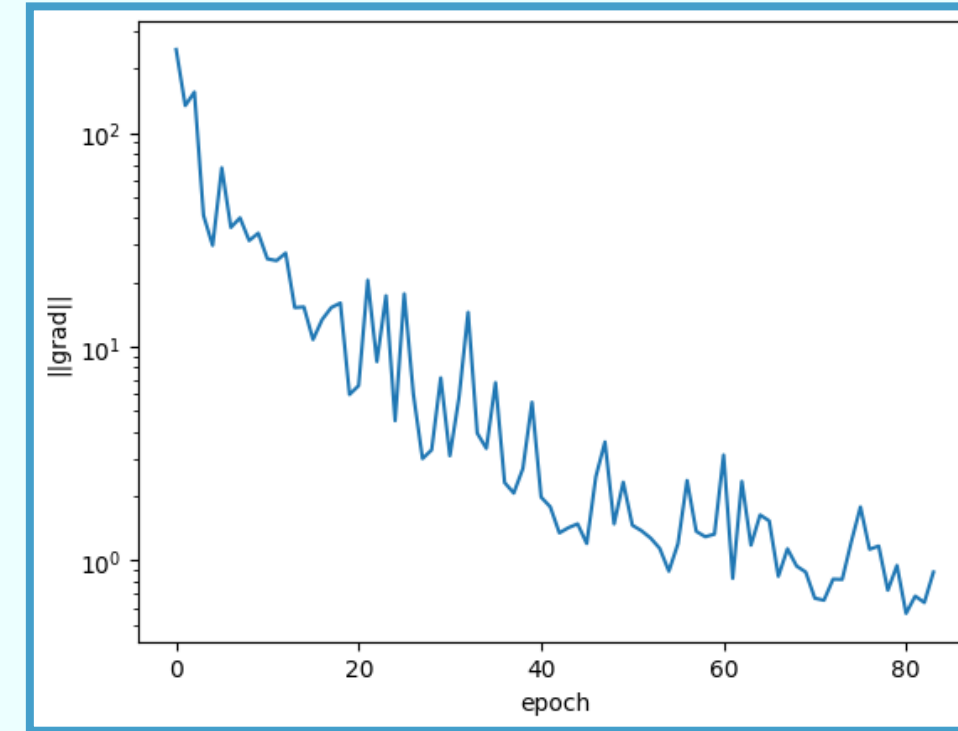


# Model stability: Closure test

## No dispersion relation (non-DR) neural model

- Pseudo-data generated from KM09
- NN learns CFFs directly  $\rightarrow$  predicts observables with  $\chi^2 \sim 1$
- The NN can learn the CFFs that the observables are sensitive to.
- The training pipeline + Gepard theory evaluation + harmonic observable machinery is working.

| Obs | $\chi^2$ |
|-----|----------|
| XLU | 1.06     |
| XUU | 1.09     |
| AC  | 1.08     |
| ALU | 0.96     |

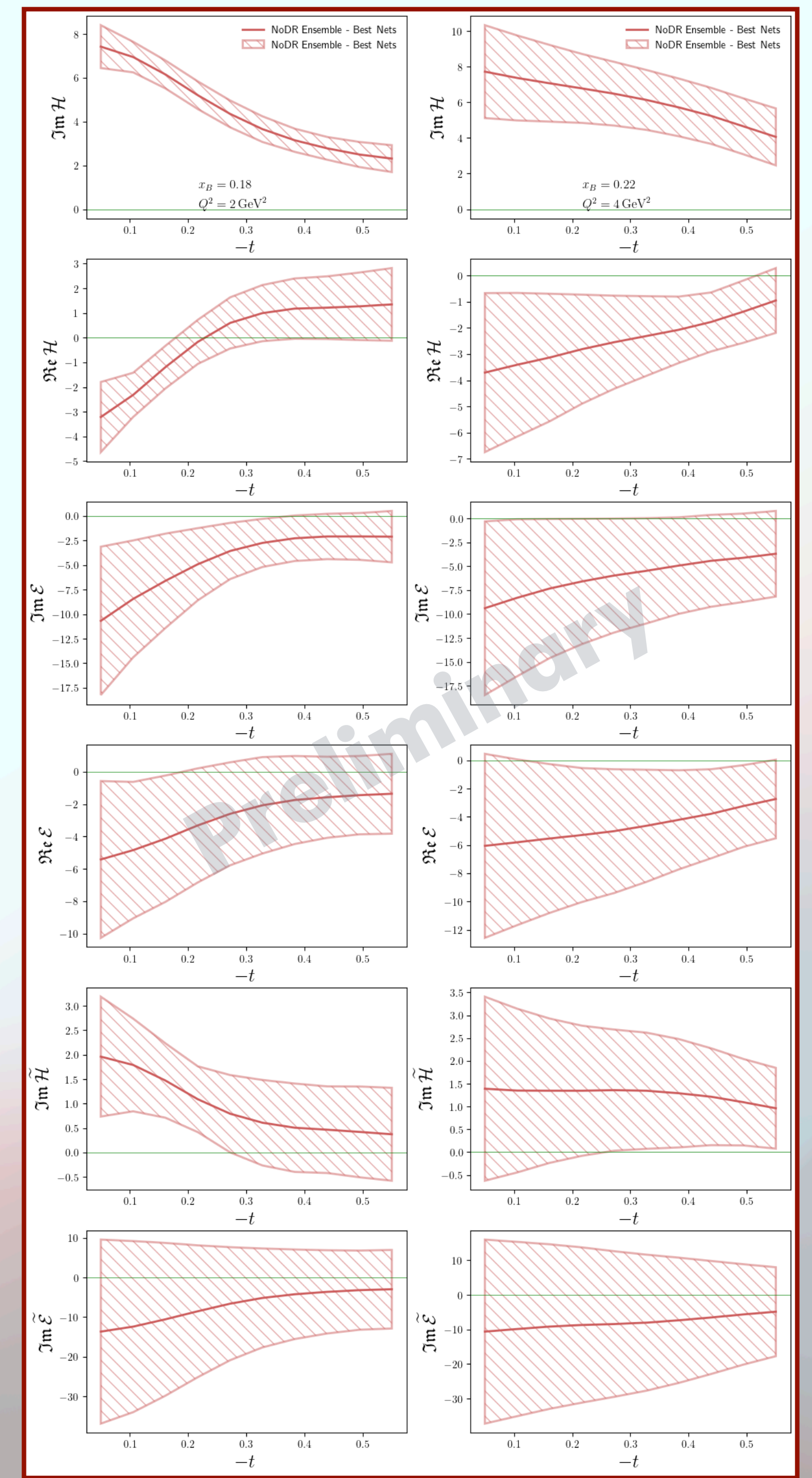
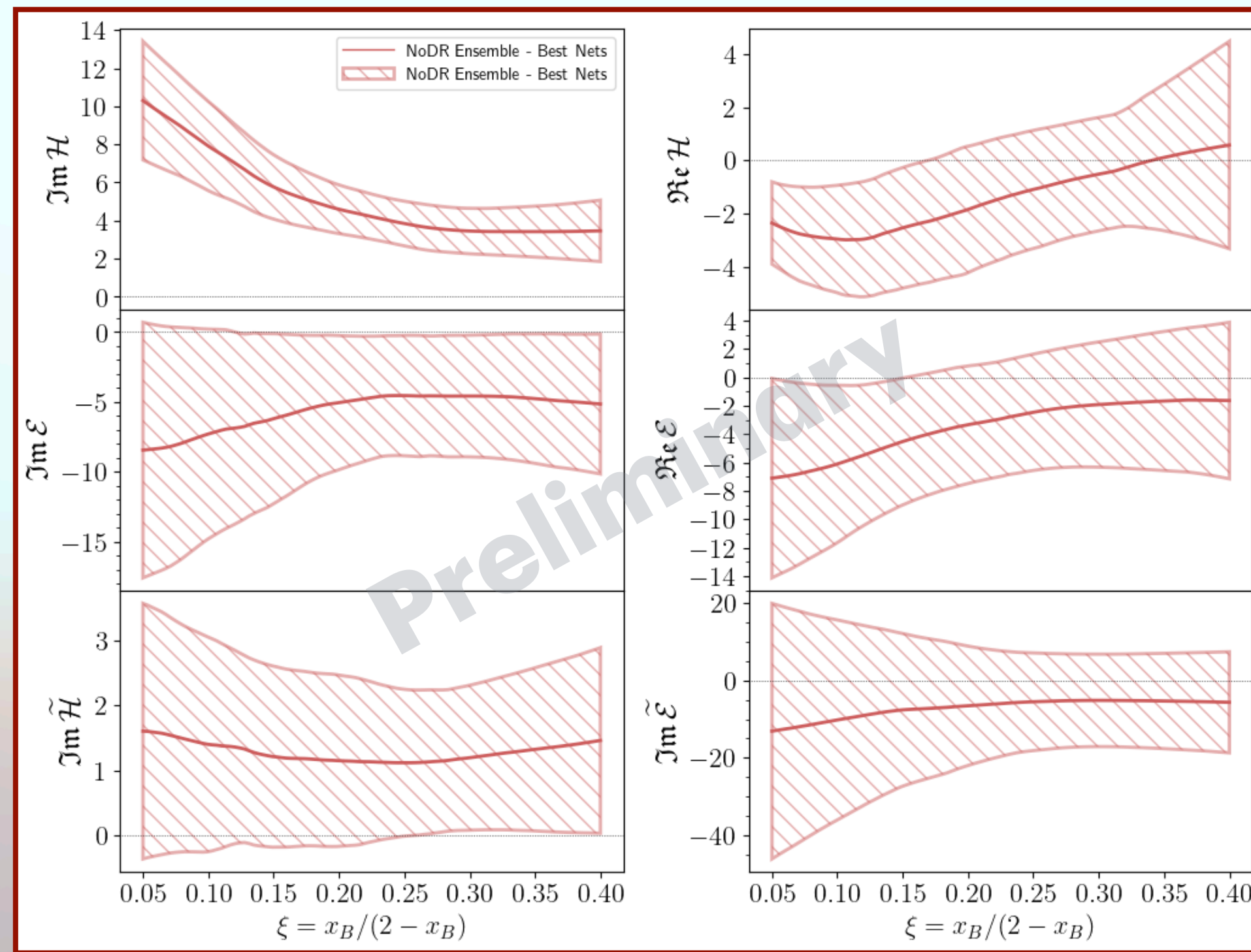


# Update on global analysis of CFFs

Dataset: CLAS + Hall A + HERMES (twist-2 safe region cut:  $-t/Q^2 < 0.25$ )

- Global non-DR fit provides stable ImH and key components. The uncertainties from ensemble spread
- We use an ensemble strategy: multiple nets/seeds  $\rightarrow$  uncertainty band reflects fit flexibility and data constraints.

| observable | collaboration | npts   | chi2_ndof |       |
|------------|---------------|--------|-----------|-------|
| 0          | ALUI          | HERMES | 6         | 4.292 |
| 1          | XUU           | CLAS   | 161       | 4.174 |
| 2          | XLUw          | HALLA  | 17        | 3.879 |
| 3          | XLU           | CLAS   | 103       | 3.192 |
| 4          | ALU           | CLAS   | 10        | 3.103 |
| 5          | BTSA          | HERMES | 4         | 2.395 |
| 6          | XUUw          | CLAS   | 320       | 2.308 |
| 7          | ALU           | CLAS   | 48        | 2.243 |
| 8          | XLUw          | HALLA  | 30        | 1.345 |
| 9          | ALU           | CLAS   | 12        | 1.250 |
| 10         | ALU           | CLAS   | 10        | 1.181 |
| 11         | BTSA          | CLAS   | 20        | 1.048 |
| 12         | XUUw          | CLAS   | 96        | 0.987 |
| 13         | XUUw          | HALLA  | 20        | 0.955 |
| 14         | AUTI          | HERMES | 4         | 0.808 |
| 15         | XUUw          | HALLA  | 44        | 0.734 |
| 16         | XLUw          | CLAS   | 48        | 0.720 |
| 17         | AC            | HERMES | 12        | 0.579 |
| 18         | TSA           | CLAS   | 10        | 0.315 |
| 19         | TSA           | HERMES | 4         | 0.285 |



# Closure test: Dispersion relation (DR) neural model

We implemented a DR-constrained neural model in Gepard

$$\text{Re}\mathcal{H}(\xi, t) = \mathcal{C}_{\mathcal{H}}(t) + \frac{1}{\pi} \text{P.V.} \int_0^1 d\xi' \left[ \frac{1}{\xi - \xi'} - \frac{1}{\xi + \xi'} \right] \text{Im}\mathcal{H}(\xi', t)$$

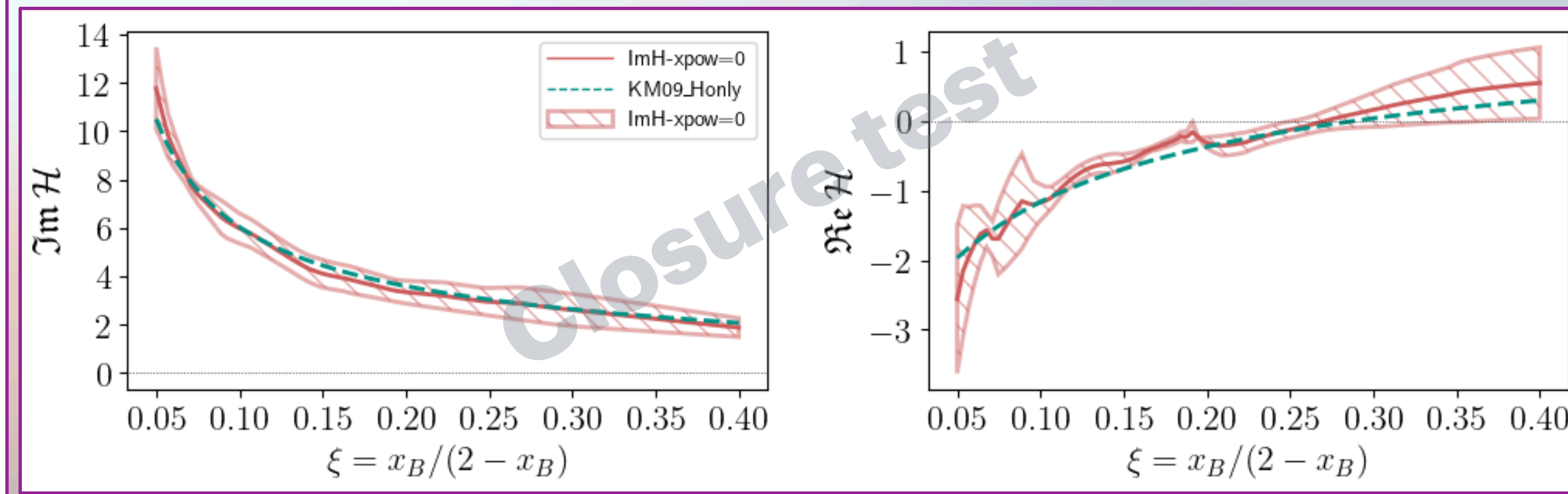
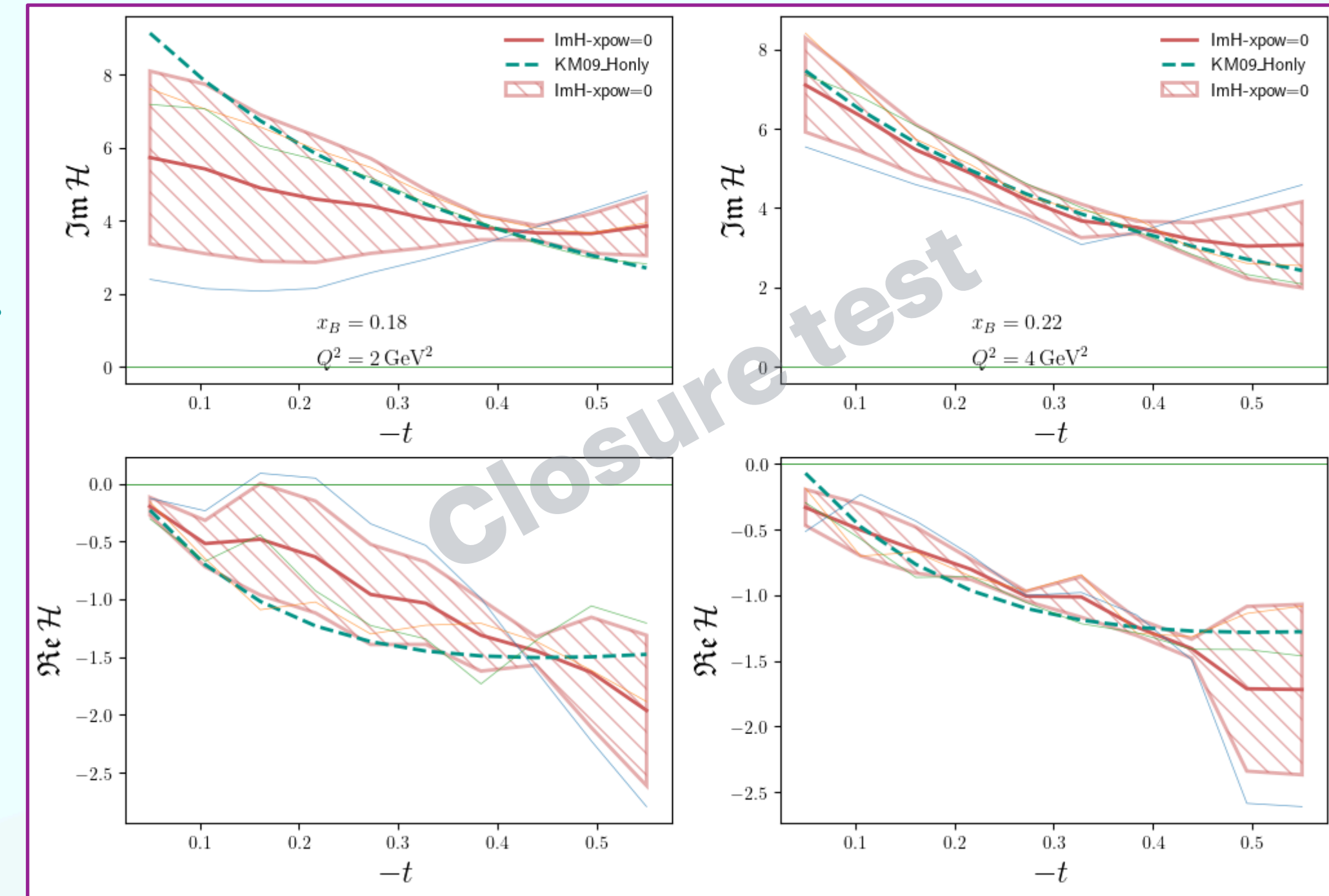
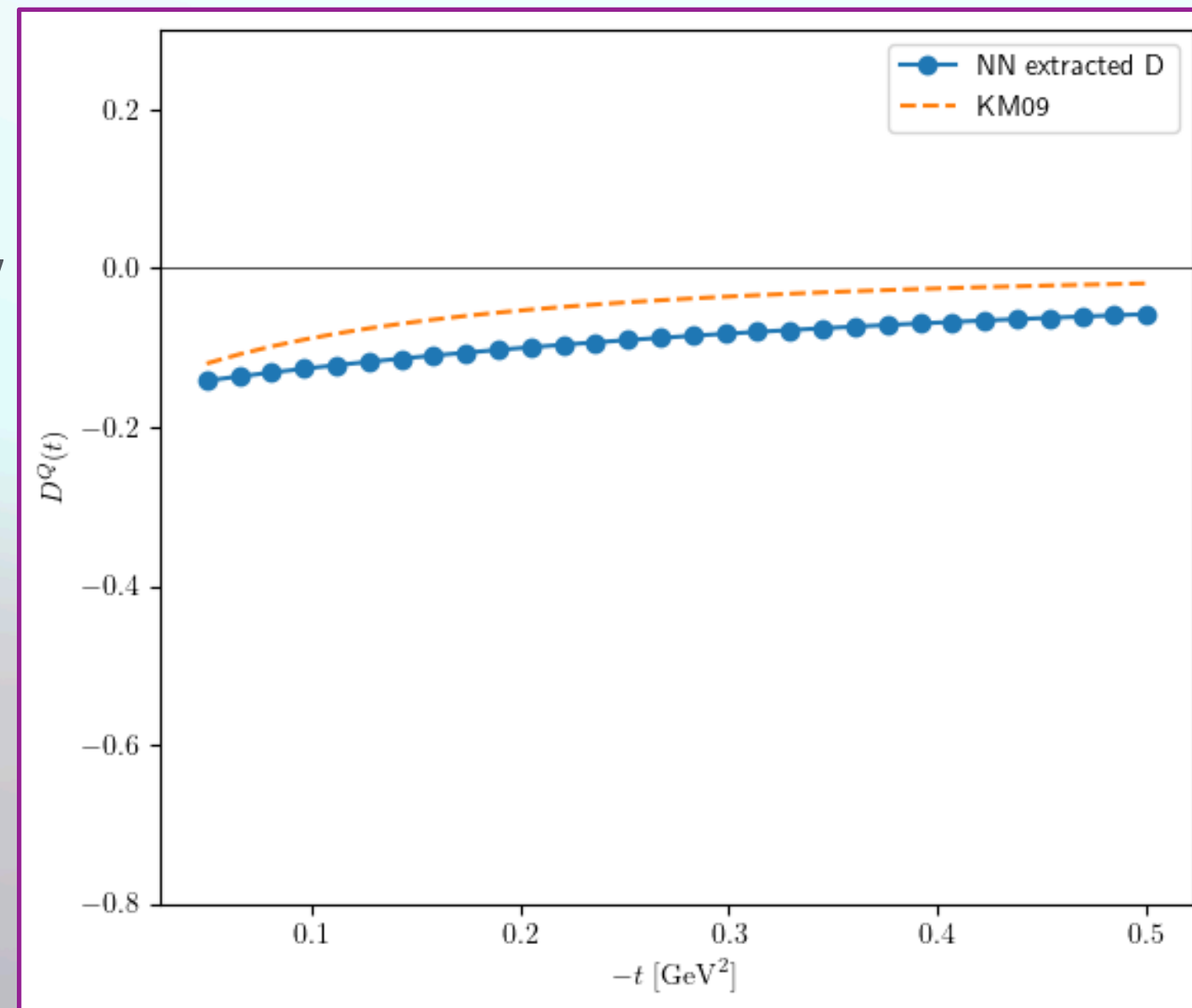
- PV integral + small- $\xi$  correct extrapolation controls ReH stability.
- D-term is still weakly constrained to be left free unless ReH-sensitive observables are ensured.

$$D(t) = \frac{D_0}{\left(1 - \frac{t}{M^2}\right)^\alpha}$$

$$D_0 = 0.2233 \quad \alpha = 2.1407$$

$$M^2 = 0.8171$$

| Obs       | $\chi^2$ |
|-----------|----------|
| XLU       | 5.5      |
| XUU       | 2.4      |
| ALU       | 15.95    |
| AUT, DVCS | 4.5      |



# Dispersion relation and D-term extraction

We implemented a DR-constrained neural model in Gepard

$$\text{Re}\mathcal{H}(\xi, t) = \mathcal{C}_{\mathcal{H}}(t) + \frac{1}{\pi} \text{P.V.} \int_0^1 d\xi' \left[ \frac{1}{\xi - \xi'} - \frac{1}{\xi + \xi'} \right] \text{Im}\mathcal{H}(\xi', t)$$

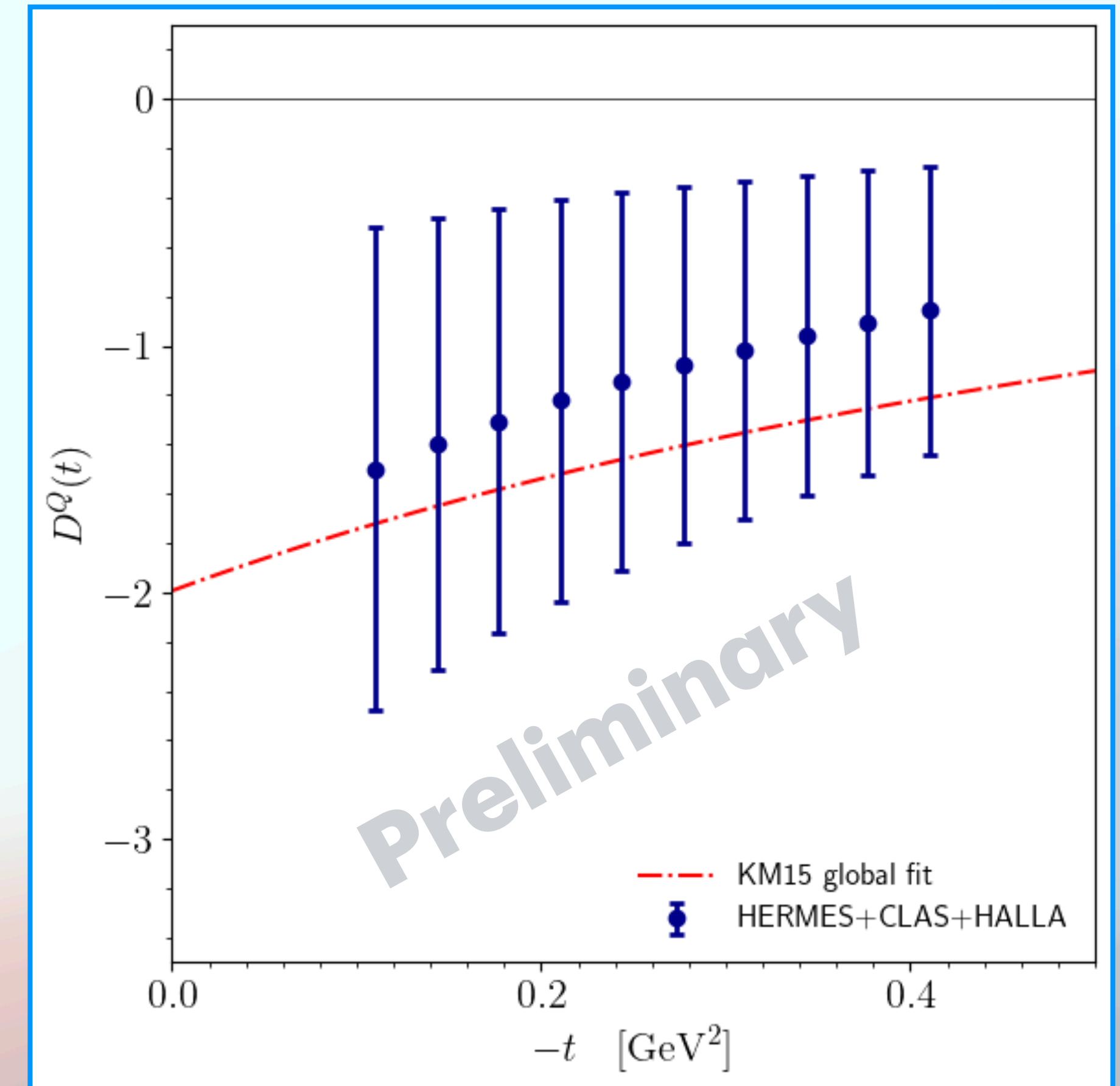
- PV integral + small- $\xi$  correct extrapolation controls ReH stability.
- D-term is still weakly constrained to be left free unless ReH-sensitive observables are ensured.

$$D(t) = \frac{D_0}{\left(1 - \frac{t}{M^2}\right)^\alpha}$$

$$D_0 = -1.2865 \quad \alpha = 2.2333$$

$$M^2 = 0.7828$$

- The preliminary global fit shows a preference for KMI5-like behavior over KM09-like behavior.



# Deliverables and future directions

# Deliverables and future directions

- Roadmap for a Global analysis: Extract harmonics for each observable, remove outliers and problematic data points, perform preliminary fit adjustments, tune hyperparameters for optimal performance, conduct ensemble analyses from several NN models and make closure tests to the created NN models.

## Deliverables:

- Global fit with consistent  $Q^2$  treatment is necessary to treat all data available.
- The DR reconstruction is extremely sensitive to the behavior of  $\text{Im}H$  outside the region directly constrained by the observables — especially the small- $\xi$  tail and the neighborhood of the principal-value point.
- We now have a validated DR-NN pipeline, and we can study D-term sensitivity in a controlled way.
- The next step is quantifying what combination of CFFs extraction and kinematic coverage makes  $D(t)$  identifiable and stable, and what priors are required.

## Future directions:

- Global fit including HERA data: Analyze the behavior change due to kinematics.
- Finish global analysis for the DR neural model.
- Create a new module on Gepard for DDVCS.
- Generate DDVCS/EIC pseudodata using EPIC and integrate into the analysis.

Thank you all for your attention

# Backup

# Database

Currently, there was no unified common database storing all available data which is necessary to reduce the uncertainties.

We developed a publicly accessible database format capable of storing current and future data as well as pseudodata.

- Stores data and pseudodata coming from various elastic and exclusive measurements and lattice-QCD results.
- Interfaces are provided in the main programming languages: Python and C++.
- Interface with GEPARD and Partons.
- Accessible by anyone in the world using Github.

Database for studying Generalised Parton Distributions (GPDs)

This page:  
[about](#)  
[installation](#)  
[data format](#)  
[basic usage](#)  
[available data](#)  
[adding new data](#)

[license](#)  
[acknowledgements](#)  
[contact](#)

View GitHub repository:  
[link](#)

View PyPI repository:  
[link](#)

View reference article:  
[arXiv](#) [inspire](#)

### Available datasets

| uuid                     | collaboration | reference   | type | pseudo | observables                                 | comment  |
|--------------------------|---------------|---|------|--------|---|--|
| <a href="#">EqbtDRkv</a> | HallA         | <a href="https://arxiv.org/pdf/1703.09442.pdf">https://arxiv.org/pdf/1703.09442.pdf</a>         | DVCS | False  | CrossSectionDifferenceLU                    | None   |
| <a href="#">PusMstKs</a> | CLAS          | <a href="https://arxiv.org/pdf/2211.11274">https://arxiv.org/pdf/2211.11274</a>                 | DVCS | False  | ALL   | None   |
| <a href="#">vGAKAf7P</a> | CLAS          | <a href="https://arxiv.org/pdf/1501.07052.pdf">https://arxiv.org/pdf/1501.07052.pdf</a>         | DVCS | False  | ALU AUL ALL                                 | None   |
| <a href="#">75ueQoQw</a> | COMPASS       | <a href="https://arxiv.org/abs/1802.02739">https://arxiv.org/abs/1802.02739</a>                 | DVCS | False  | CrossSectionUUVirtualPhotoProduction TSlope | None   |
| <a href="#">ob8hLTm2</a> | CLAS          | <a href="https://arxiv.org/pdf/1810.02110">https://arxiv.org/pdf/1810.02110</a>                 | DVCS | False  | CrossSectionUU                              | Differential CrossSection for exclusive DVCS electroproduction |
| <a href="#">3gYp9R4P</a> | HERMES        | <a href="https://arxiv.org/pdf/hep-ex/0605108.pdf">https://arxiv.org/pdf/hep-ex/0605108.pdf</a> | DVCS | False  | AcCos1Phi                                   | None   |
| <a href="#">bmTzHHvg</a> | HallA         | <a href="https://arxiv.org/pdf/2109.02076">https://arxiv.org/pdf/2109.02076</a>                 | DVCS | False  | CrossSectionUU                              | Beam-helicity-independent cross section                        |
| <a href="#">RQncbKtk</a> | CLAS          | <a href="https://arxiv.org/pdf/1504.02009v1.pdf">https://arxiv.org/pdf/1504.02009v1.pdf</a>     | DVCS | False  | CrossSectionUU CrossSectionDifferenceLU     | None   |
| <a href="#">AtY8o7Ej</a> | HallA         | <a href="https://arxiv.org/pdf/1504.05453v1.pdf">https://arxiv.org/pdf/1504.05453v1.pdf</a>     | DVCS | False  | CrossSectionUU CrossSectionDifferenceLU     | None   |

In collaboration with P. Sznajder and C. Mezrag

[arxiv.org/abs/2503.18152](https://arxiv.org/abs/2503.18152)

<https://opengpd.github.io/gpddatabase/index.html>

# Database

Currently, there was no unified common database storing all available data which is necessary to reduce the uncertainties.

We developed a publicly accessible database format capable of storing current and future data as well as pseudodata.

- Get the list of available data files.
- Load a given data file
- Get metadata.
- Upload your own data file for the use of the GPD community.

Database for studying Generalised Parton Distributions (GPDs)

This page:  
[about](#)  
[installation](#)  
[data format](#)  
[basic usage](#)  
[available data](#)  
[adding new data](#)

[license](#)  
[acknowledgements](#)  
[contact](#)

View GitHub repository:  
[link](#)

View PyPI repository:  
[link](#)

View reference article:  
[arXiv](#) [inspire](#)

### Available datasets

| uuid                     | collaboration | reference   | type | pseudo | observables                                 | comment  |
|--------------------------|---------------|---|------|--------|---|--|
| <a href="#">EqbtDRkv</a> | HallA         | <a href="https://arxiv.org/pdf/1703.09442.pdf">https://arxiv.org/pdf/1703.09442.pdf</a>         | DVCS | False  | CrossSectionDifferenceLU                    | None   |
| <a href="#">PusMstKs</a> | CLAS          | <a href="https://arxiv.org/pdf/2211.11274">https://arxiv.org/pdf/2211.11274</a>                 | DVCS | False  | ALL   | None   |
| <a href="#">vGAKAf7P</a> | CLAS          | <a href="https://arxiv.org/pdf/1501.07052.pdf">https://arxiv.org/pdf/1501.07052.pdf</a>         | DVCS | False  | ALU AUL ALL                                 | None   |
| <a href="#">75ueQoQw</a> | COMPASS       | <a href="https://arxiv.org/abs/1802.02739">https://arxiv.org/abs/1802.02739</a>                 | DVCS | False  | CrossSectionUUVirtualPhotoProduction TSlope | None   |
| <a href="#">ob8hLTm2</a> | CLAS          | <a href="https://arxiv.org/pdf/1810.02110">https://arxiv.org/pdf/1810.02110</a>                 | DVCS | False  | CrossSectionUU                              | Differential CrossSection for exclusive DVCS electroproduction |
| <a href="#">3gYp9R4P</a> | HERMES        | <a href="https://arxiv.org/pdf/hep-ex/0605108.pdf">https://arxiv.org/pdf/hep-ex/0605108.pdf</a> | DVCS | False  | AcCos1Phi                                   | None   |
| <a href="#">bmTzHHvg</a> | HallA         | <a href="https://arxiv.org/pdf/2109.02076">https://arxiv.org/pdf/2109.02076</a>                 | DVCS | False  | CrossSectionUU                              | Beam-helicity-independent cross section                        |
| <a href="#">RQncbKtk</a> | CLAS          | <a href="https://arxiv.org/pdf/1504.02009v1.pdf">https://arxiv.org/pdf/1504.02009v1.pdf</a>     | DVCS | False  | CrossSectionUU CrossSectionDifferenceLU     | None   |
| <a href="#">AtY8o7Ej</a> | HallA         | <a href="https://arxiv.org/pdf/1504.05453v1.pdf">https://arxiv.org/pdf/1504.05453v1.pdf</a>     | DVCS | False  | CrossSectionUU CrossSectionDifferenceLU     | None   |

In collaboration with P. Sznajder and C. Mezrag

[arxiv.org/abs/2503.18152](https://arxiv.org/abs/2503.18152)

<https://opengpd.github.io/gpddatabase/index.html>

# Accessing GFFs

Considering some assumptions like:

1. At LO, gluons don't contribute to DVCS much, so one can assume that the subtraction constant is dominantly coming from quarks, but for the moment, we also neglect strange and heavier quarks.
2. To talk about “quark pressure,” one needs to neglect energy-momentum flow from quarks to gluons described by the EMT form factor  $\tilde{C}(t)$ .
2. In the asymptotic limit  $d_n^q(t)$  vanish for  $n > 1$ . Where  $d_1^q(t)$  determine the asymptotic form of the GPDs.
3. Considerate the dominance of the flavor singlet combination.

To date, a more conservative extraction of the subtraction constant from the currently available experimental data remains compatible with zero within large uncertainties.

By utilizing this DR, along with other phenomenological assumptions, we can extract the CFFs and GFFs from experimental data and enhance the results with lattice calculations!

$$\Delta(t) = 2 \sum_q e_q^2 \int_{-1}^1 dz \frac{D_{\text{term}}^q(z, t)}{1 - z},$$

$$d_1^u = d_1^d = d_1^Q / 2$$

$$D_{\text{term}}^q(z, t) = (1 - z^2) \sum_{\text{odd } n} d_n^q(t) C_n^{3/2}(z)$$

$$D_q(t) = \frac{4}{5} d_1^q(t) = \int_{-1}^1 dz z D_{\text{term}}^q(z, t)$$

$$\Delta(t) = 4 \left( \frac{4}{9} d_1^u(t) + \frac{1}{9} d_1^d(t) \right)$$

$$D^Q(t) = \frac{18}{25} \Delta(t).$$

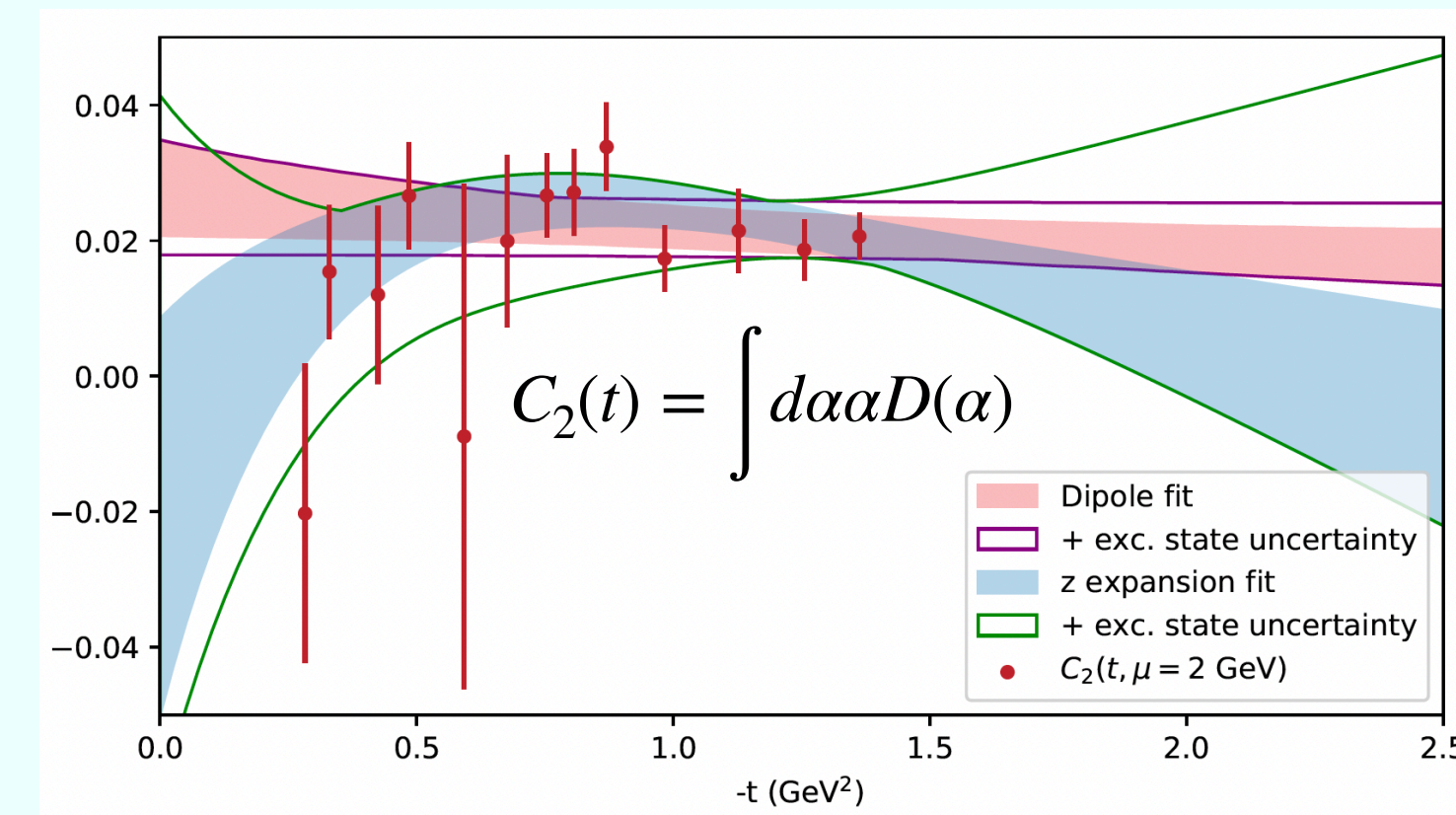
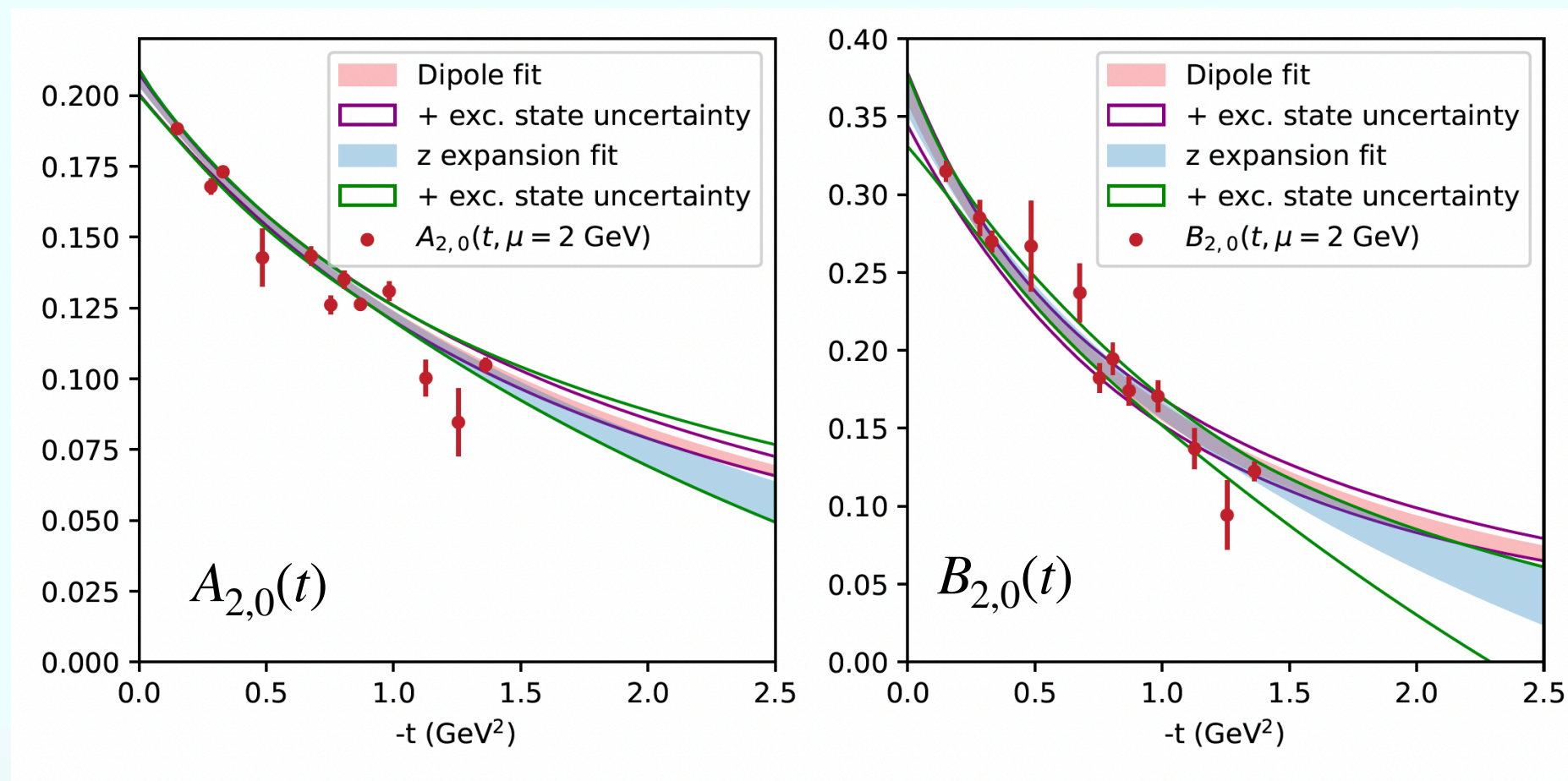
# State of the project: Inputs from Lattice QCD

$$D_{\text{term}}^q(z, t) = (1 - z^2) \sum_{\text{odd } n} d_n^q(t) C_n^{3/2}(z)$$

Lattice QCD (LQCD) constraints can help reduce the large systematic uncertainties in GFF extractions by accounting for higher-order terms in Gegenbauer expansions.

## Extraction of the isovector GFFs from Lattice QCD

I.J. High Energy Phys. 2024, 162 (2024)



- Calculation of the non-singlet “ $u - d$ ” combination of GFF, which cannot be probed through DVCS, has been performed in Lattice across a wide range of  $t$ .
- To fully constrain the analysis, isoscalar GFFs (connected contributions) are also needed.

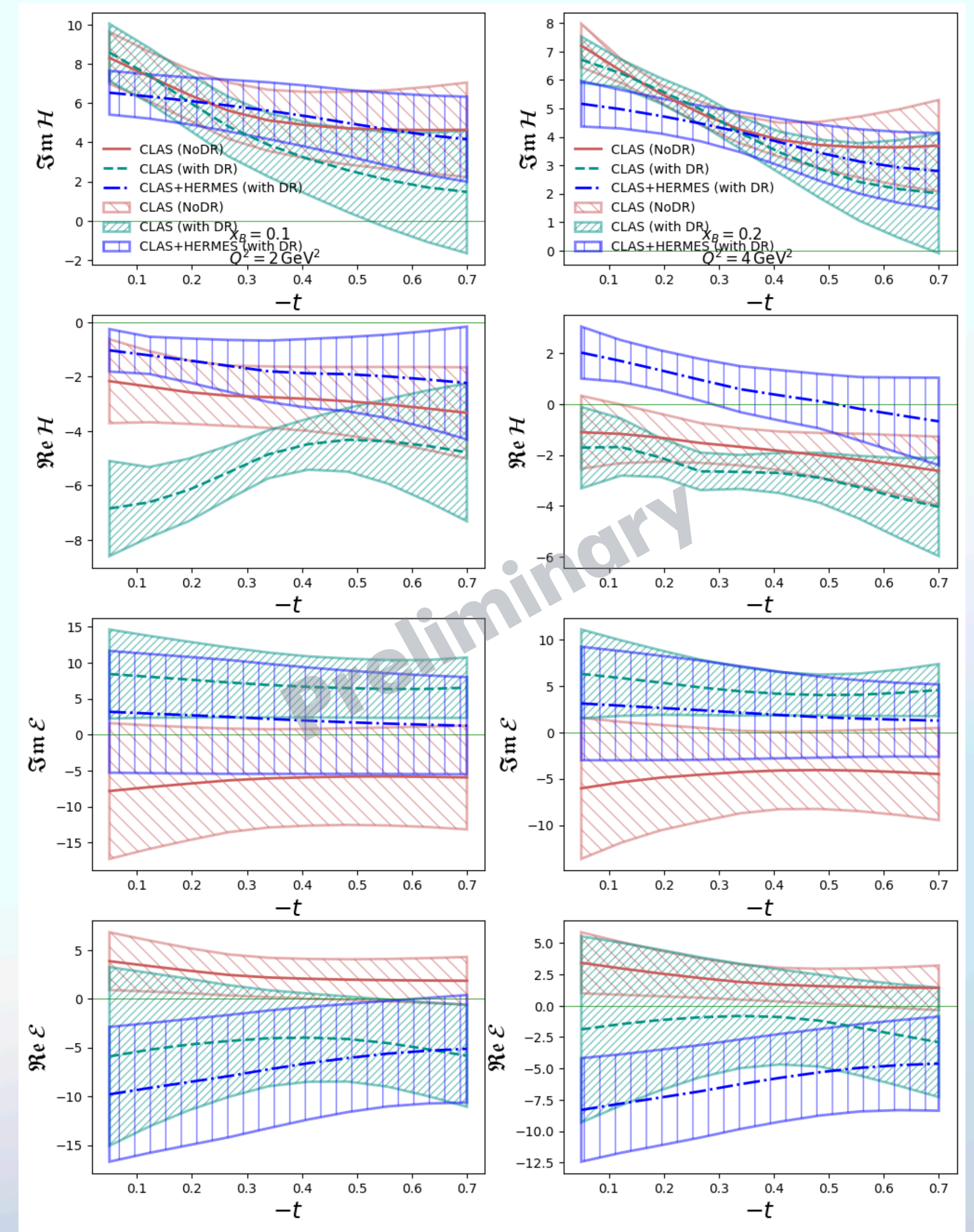
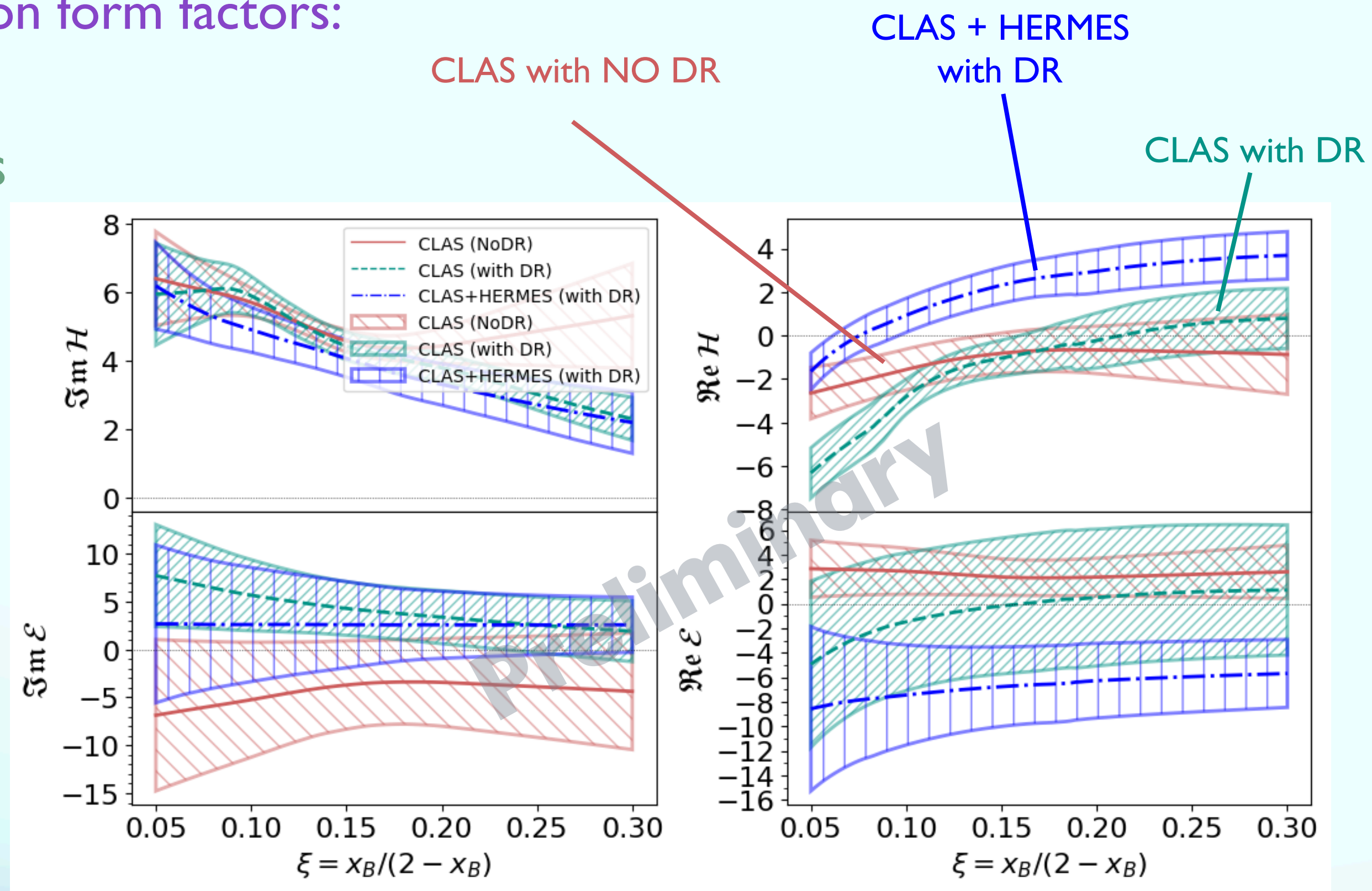
## How can we use this data in a Global analysis?

- Lattice calculations can provide direct information about CFF.
- Plan to merge LQCD-derived CFFs into the neural network fitting framework, complementing experimental data and improving constraints in the loss function.

# Preliminary fits

Compton form factors:

4 CFFs



CLAS BSA at  $\sim 11$  GeV data (Phys. Rev. Lett. 130, 211902) raise the range of kinematic restrictions

$$\chi^2/dof = 1.34$$

Planning to add the upcoming CLAS cross-section data.